12-2018

PRIORITIZING CHEMICAL CONSTITUENTS IN TOBACCO PRODUCTS AND SMOKE TO PREDICT DEVELOPMENTAL OSTEOTOXICITY IN HUMAN EMBRYONIC STEM CELLS

Joseph Madrid
joseph.madrid@csusb.edu

PRIORITIZING CHEMICAL CONSTITUENTS IN TOBACCO PRODUCTS AND SMOKE TO PREDICT DEVELOPMENTAL OSTEOTOXICITY IN HUMAN EMBRYONIC STEM CELLS

A Thesis

Presented to the

Faculty of

California State University,

San Bernardino

In Partial Fulfillment

of the Requirements for the Degree

Master of Science in

Biology

by

Joseph Valenzuela Madrid

December 2018

PRIORITIZING CHEMICAL CONSTITUENTS IN TOBACCO PRODUCTS AND SMOKE TO PREDICT DEVELOPMENTAL OSTEOTOXICITY IN HUMAN EMBRYONIC STEM CELLS

A Thesis

Presented to the

Faculty of

California State University,

San Bernardino

---

by

Joseph Valenzuela Madrid

December 2018

Approved by:

Dr. Nicole Bournias, Committee Chair, Biology

Dr. Nicole zur Nieden, Committee Member, UCR, Biology

Dr. Jeffrey Thompson, Committee Member

ABSTRACT

Though it is well known that tobacco related products can cause prenatal maldevelopment, very little is known on how tobacco products affect bone tissue as it develops in the embryo. Identifying which chemicals can induce the greatest harm to the prenatal skeletal system is an improbable task as there are over 7,000 chemicals in tobacco smoke alone. We hypothesized that the Toxicological Priority Index (ToxPI) program can be used to rank osteogenic cytotoxicity potential to aid in the assessment of what chemicals out of the thousands can cause osteogenic differentiation inhibition. ToxPI aggregates information from various assays and incorporates them into visual “pie charts” which allow chemicals to be ranked against each other by given parameters. The larger the pie chart the greater likelihood of potential effects and vice versa. Seventeen tobacco chemical constituents were ranked using ToxPI and those chemicals with pie charts (0<X) are predicted to have decreased cell viability and differentiation capabilities where chemicals with null pie charts (x=0) will not have any effects.

To assess the ability of ToxPI to correctly predict maldevelopment *in silico* eight compounds were then tested in vitro: four of them being ToxPi positive and the other four having null predicted effects. To verify the predictions, human embryonic stem cells were differentiated into osteoblasts and exposed to various concentrations of each compound. Cell viability was measured via MTT assay in conjunction with a calcium assay to measure osteogenic differentiation. In

addition, adult human feeder fibroblasts cell viability in response to exposure was measured. ToxPI positive predictions (x<0) all exhibited decreased cell viability though in various order. All tested ToxPI null charts produced no change in cell viability. However, one of the ToxPI null chemicals, nicotine, although not cytotoxic *in vitro*, caused differentiation inhibition. Together our data suggests that ToxPi might be useful to identify strongly inhibitory chemicals based on their cytotoxicity but might also give false negative results for chemicals that cause differentiation inhibition at sub-toxic levels.

ACKNOWLEDGEMENTS

I would like to acknowledge Dr. Nicole Bournias for giving me the opportunity to attend graduate school. You have greatly impacted my life moving forward by giving my science education a much-needed jump start. I owe a large amount of gratitude to Dr. Nicole zur Nieden who has been my PI for the last three years. I appreciate all her guidance, knowledge, and most importantly the patience she has graciously bestowed upon me. Special thanks to Dr. Jeffrey Thompson for being a part of my thesis committee. His willingness to take time out his day to help me solve issues were beyond valuable.

I wish to thank all current and past members of the zur Nieden lab. Specifically, Nicole Sparks who's had to deal with antics daily and has been a guiding force in my career. She has been my Noah's Ark in the tumultuous sea known as graduate school. I couldn't have done this without you. Thank you, Lauren Walker, for being a great friend and teammate. Not only are you the Beyoncé of Biology, but you were always there to listen to me complain and consistently reminded me I had the power to change my problems.

Thank you to the California Institute for Regenerative Medicine for funding this research. The CSUSB Biology department has also given me a plethora of opportunities and I am eternally grateful. Thank you, Debbie Reynolds, for allowing me to distract you, for hours at a time, by sitting and ranting on your office couch. A thank you to my collaborator at UCR, Dr. David Volz and his accompanying laboratory team.

I would like to thank the Madrid and Valenzuela family for the unwavering downpour of love and support I have received throughout my life. Thank you to my grandparents, who have been sources of inspiration and hope in my life. A loving thanks to my mother and father who were brave enough to let me find my own way in life. A thank you to my siblings and their respective families, because being a brother and an uncle to my nieces, Haley, Brooklyn, and Lupine have always been the consistent joy of my life.

Special thanks to all my friends, who I owe a large amount of praise. Thank you to Don'Shawn Cato, who has been my closest friend for about a decade. Friendships like yours only come once in a lifetime. The Barrino, Fanale, and Ortiz family who at various points over the last three years offered me a home, I am forever grateful for the generosity and kindness you gave me, even when I didn't deserve it.

Lastly, thank you to Shannon Kim, who was by my side for a majority of my graduate school journey. I truly hope you find peace and happiness in your life.

DEDICATION

In loving memory of Henry Jesus Madrid and Jose Robles Valenzuela.

“Woe to philosophers [people] who cannot laugh away their wrinkles, I look upon solemnity as a disease” - Voltaire

TABLE OF CONTENTS

LIST OF TABLES

LIST OF FIGURES

CHAPTER ONE

INTRODUCTION

Health Consequences of Exposure to Tobacco

The environment plays a prominent role in human health as it could negatively impact all stages of life. The World Health Organization (WHO) estimates 24% of the global disease burden and 23% of all deaths to be attributed to environmental factors.[1] Environmental factors can come in the means of biological, chemical, and radioactive substances. For instance, continuous use of medications such as valproate have been associated with short stature[2], and supplemental addition of retinoic acid in the diet of a pregnant mother has been linked to craniofacial abnormalities.[3] With the potential to alter and harm human health it is of great importance to study and assess a chemical's range of potential outcomes in the absence of an acquired disease or genetic predisposition.

The most common environmental and indoor toxicant is exposure to smoke via cigarettes. Such exposure can be through mainstream smoke (MS) that is actively inhaled by the user, side stream smoke (SS), which burns off the ends of cigarettes, and third hand smoke (THS) that consists of left-over particulate matter that can rest in clothing, carpets, and any outdoor or indoor surfaces. In addition, exposure can happen orally through use of noncombustible tobacco products such as chewing tobacco. All these tobacco products are

known to cause a broad spectrum of health effects. In adults, its use is associated with an increased risk of gum disease, blindness, reduced fertility in addition to respiratory complications and cardiovascular disease. Smoking is strongly associated with cancers that are not limited to the head, neck, lung, bladder, stomach, and colon.[4] Tobacco products overall will reduce human health: if every smoker decided to stop smoking, one in three cancer deaths would cease to exist.[3] The Center for Disease Control (CDC) estimates that one in five deaths in the United States can be attributed to cigarette smoking and is responsible for 480,000 deaths annually.[4] In addition to disease, the total economic cost of smoking is 300 billion dollars a year in the United States alone.[5] Exposure to tobacco products can also induce tissue specific effects as seen in adult bone. Smoking has been shown to disrupt osteogenesis and can lead to osteoporosis, an increase in bone fragility, and an overall delay in bone healing.[6]

Despite these known health consequences of tobacco use, 10-20% of pregnant women report smoking during their first trimester of pregnancy.[7] Smoking during pregnancy is linked to premature birth, sudden infant death syndrome, low birth weight, and ectopic pregnancy[4], but whether tobacco exposure is harmful to the developing skeleton is understudied. However, perpetrating bone growth and density could have irreversible effects on the development of the fetus and pose a significant threat to the baby's health postpartum as evidence suggests skeletal growth is programmed very early in development. In fact, a few years ago, Rasmussen reported that while tobacco

exposure may not lead to premature death, it can still perturb development to cause a birth defect.[8]

Skeletal Development

The skeleton protects critical organs such as the brain in addition to providing a scaffold, which the body rests upon. The axial skeleton provides the core of the skeletal system and consists of the spinal column, and ribcage. The appendicular skeleton encompasses the extremities of the skeletal system, but also include the pelvic and pectoral girdle along with the clavicles. Skeletal development post fertilization starts from anterior to posterior, essentially starting from the skull descending to the spinal column while filling out the rib cage. The extremities of the body develop from the pelvic and pectoral girdles and extend out laterally.[9] Two bone development processes are responsible for formation of the skeleton: intramembranous and endochondral ossification. Neural crest derived mesenchymal precursors undergo intramembranous ossification, which is a direct bone formation process. Parts of the skull and clavicles develop bone through intramembranous ossification. Cells from a mesoderm mesenchymal origin use endochondral ossification that uses a temporary cartilage placeholder that is eventually replaced with bone, as seen in many long bones. The appendicular skeleton and base of the skull is primarily produced via this type of ossification.[10] Once developed, osteoblasts, the bone forming cells, and osteoclasts, which resorp the bone matrix, are the predominant cell types in bone

and their interaction drives bone remodeling. The skeleton is continuously restructured and grows in both diameter and length post birth continuing into adolescence.[11]

Developmental Biology

Developmental biology studies the initiation and construction of the organism as a developing embryo. This is contrary to other fields of biology that focus on maintenance and repair of adult organisms. Studying embryonic development can help shed light on the process of how organisms differentiate, organize, and grow before birth. This transient stage between egg and sperm into a functioning organism is critical as this developmental period is relatively quick and short. During this limited time frame a major question of how environmental cues impact the developmental process needs to be assessed.

Most mammal keep their embryos inside of themselves and exposure to environmental agents through the mother will impact the development of the embryo as well. This is a major concern as the use of chemicals has increased in various sectors of transport, agriculture, and industry. WHO estimates that 47,000 deaths annually can be directly attributed to chemical exposure. In the absence of fatal exposure, teratogens are of great concern. Teratogens are agents that can disturb development of the embryo and produce a birth defect. This is especially alarming as the number of birth defects have been increasing in the United States by 150,000 a year.[12] These defects have ranged from limb

reduction, cardiac malformation and impaired neural development. In summary, the study of development is necessary, as it adds depth to other biological disciplines such as cell biology, anatomy, and genetics.

Embryonic Stem Cells

Embryonic stem cells (ESCs) are unspecialized pluripotent cells, that give rise to all specialized cells within the body (Figure 1). This pluripotency allows ESCs to differentiate into the three germ layers (endoderm, mesoderm, ectoderm), which encompass over 200 cell types.[13] However, ESCs do not give rise to extraembryonic tissues, such as the placenta, and can only develop the embryo proper. Derived from the inner cell mass of the blastocyst at day 5 post fertilization, ESCs can be isolated and plated to grow in laboratory conditions. In culture, ESCs self-renew and replicate themselves into the same non-specialized cell continuously for long periods of time, a state that is maintained by the presence of a triad of transcription factors composed of OCT4, SOX2, and NANOG, which co-occupy regions of ESC chromatin to activate pluripotency genes and repress differentiation genes.[14,15]

With the suppression of pluripotency markers, it is possible for ESCs to begin to differentiate into other cell types. In a non-adherent environment, ESCs can be forced to aggregate and form embryoid bodies, which contain differentiating cells of all three germ layers. The aggregation of ESCs in suspension is commonly referred to as the hanging drop method. When plated

on an adherent surface, embryoid bodies spontaneously differentiate into a variety of cell types, one of the most prominent being cardiomyocytes that can contract with synchronistic rhythmic activity.[16] To help drive ESCs to other cell lineages and fates chemicals can be supplemented in culture.

The potential use of ESC is a remarkable tool that allows predictability through *in vitro* results. Murine ESC have been harvested and used since 1981 but it was not until the late 1990s that the first human stem cells were isolated.

Adult stem cells differ from ESC as their differentiation potential to produce the germ layers of the body is limited and reduced to certain organs or tissues due to the pluripotency transcription triad being altered or absent. Due to this limited differentiation potentially, adult stem cells are considered multi- or uni-potent. In addition to a reduced amount of lineage potential, adult stem cells do not have unlimited proliferative potential and do have a finite limit to replace cells. With the limited ability to create certain cell types adult stem cells are only able to differentiate and replace those tissues from where they are found. So far adult stem cells have been found in mesenchymal, hematopoietic, and neural tissues.[17]

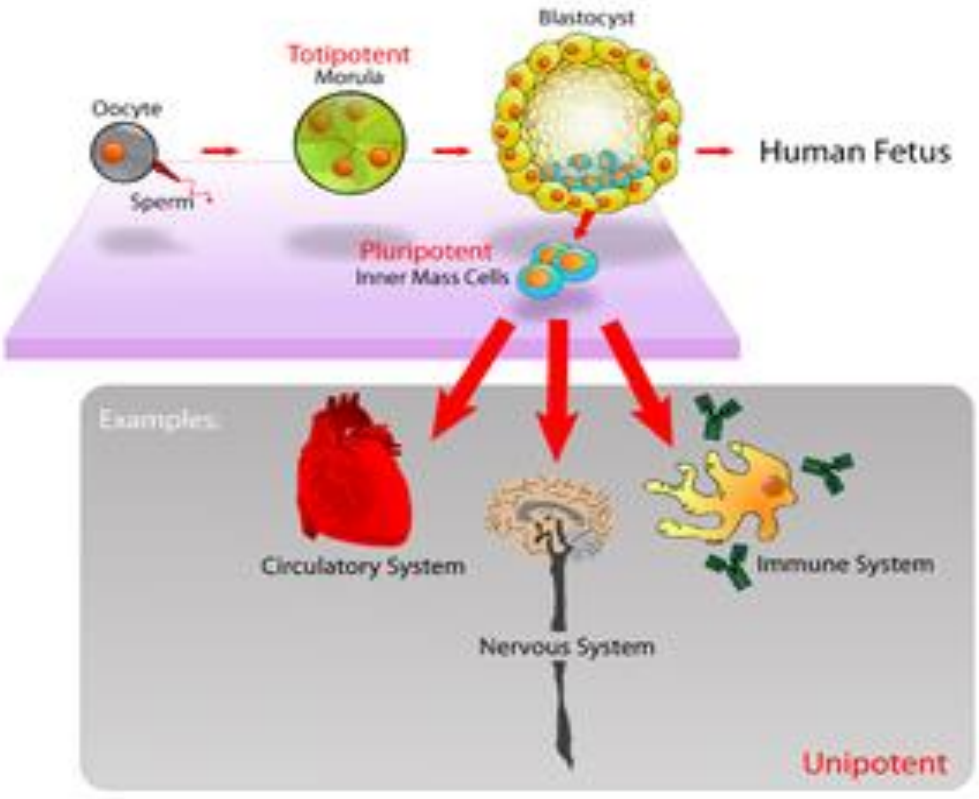

Figure 1. Pluripotency of Embryonic Stem Cells. ESCs can differentiate to all 3 germs layers. Several key transcription factors control stem cell pluripotency and renewal. With the suppression of pluripotency markers and supplementation of chemical factors ESC can be pushed to a certain cell lineage in vitro. Embryonic Stem Cell [Pluripotent: Embryonic stem cells are able to develop into any type of cell, excepting those of the placenta. Only embryonic stem cells of the morula are totipotent: able to develop into any type of cell, including those of the placenta.]. (n.d.). Retrieved December 22, 2017, from https://en.wikipedia.org/wiki/Embryonic_stem_cell

Embryonic Stem Cell Test

To limit human exposure risk to hazardous environmental chemicals and drugs, chemical compounds have been historically screened in rodents. However, since the mid-20th century there has been a push to reduce the amount of animal use and suffering for scientific purposes. The concept of the

Three R's (Replacement, Reduction, and Refinement) outlined the importance of refraining from animal use and when possible use *in vitro* and projection models to perform experiments.[18,19] A cellular approach allows safe, reliable, and high throughput results. Three such approaches based on cells, the micromass whole cell culture assay, the FETAX test (Frog Embryo Teratogenesis Assay-Xenopus), and the Embryonic Stem Cell Test (EST)[20] were validated in 2002 by the European Centre for Validation of Alternative Methods (ECVAM) for accuracy and predictivity. While all three were found potentially useful, only the EST avoided the use of animal testing entirely. In addition to avoiding the sacrificial use of animals, the EST is less laborious than other *in vitro* techniques and requires less technical skill.

To classify potentially embryotoxic compounds the EST uses three endpoints: i) Viability of 3T3 adult cells ii) viability of ESCs iii) differentiation capability of ESCs to cardiomyocytes. ESCs are a good model for development as gene expression during spontaneous differentiation into cardiomyocytes *in vitro* mimics development *in utero*. Cell viability of cardiomyocytes is measured via the MTT indirectly through metabolic activity, whereas differentiation is determined by the amount of beating clusters using microscopy. Dose response curves are developed, and half maximal activity is recorded for cytotoxicity (IC_{50}) and differentiation inhibition of cardiomyocytes (ID_{50}). These results are then incorporated into a bio-statistical model, where compounds and chemicals can be classified into three categories based on their ability to induce developmental

toxicity: Strongly embryotoxic, weakly embryotoxic, and non-embryotoxic.[21,22] Validation studies on the EST to classify embryo-toxins compared *in vitro* to *in vivo* data and found the EST had a 78% correct classification for the tested compounds.

Improvement to the EST

The classical EST used cardiomyocytes as their differentiation capabilities were spontaneously generated *in vitro*, though some exogenous factors can have effects on specific tissues such as the central nervous system and leave other organ and tissues unharmed.[23] To expand the usefulness of the EST, protocols to differentiate ESCs into a variety of tissues including neural, adipose, and bone, were then subsequently developed.[24,25]

The zur Nieden lab has been instrumental in developing differentiation protocols to drive cell commitment of human and murine embryonic stem cells into chondrocytes and osteoblasts.[24-26] To initiate differentiation, murine ESCs are switched to culture conditions from which pluripotency factors are omitted. Subsequent supplementation with the osteogenic specific factors $1,25(OH)_2$ vitamin D_3, β-glycerophosphate and ascorbic acid sends the cells down an osteogenic path, during which the cells express a variety of bone markers in sequence mimicking embryonic bone development. The final phenotypic appearance of osteoblasts in culture is characterized by black appearing deposits, which are made up of calcium.[27]

To improve the EST, additional technical endpoints were added such as

RT-PCR and flow cytometry to concentrate on genes necessary for differentiation into a specific cell lineage and standardize read-out.[28] Another added benefit of such techniques is that monitoring gene and protein expression can assess real time regulation and provide temporal data specific for each chemical.

More recent alterations to the classical EST included the animal model used in the experiment. The classical EST uses murine ESCs, though the use of primate stem cells could abrogate the differences between species that have been reported in toxicological studies. Zur Nieden and colleagues have provided evidence that primate and human cells used in the EST are more sensitive to certain compounds than their murine counterparts.[29] In addition, the murine to human switch also provides an additional advantage as human cells do not require embryoid bodies to form during the experimental process. Human ESCs can be grown and plated directly into culture plates, which allows less intrusion during the experiment and eliminate the technically and laborious task of performing the hanging drop method. Additionally, mature cell line used in the EST was switched from mouse 3T3 cells to human foreskin fibroblasts (hFFs) to better mimic the mother's toxicological response during pregnancy.

Toxicology Priority Index

To prioritize chemicals for toxicity testing the Environmental Protection Agency (EPA) in conjunction with the University of South Carolina at Chapel Hill developed the Toxicology Priority Index (ToxPI) Graphical User Interface using

data from aggregated database sources such as the EPA's Tox21 and Toxcast. The ToxPI system is a free downloadable prioritization support tool that can evaluate the toxicity of a given chemical based on various sources of data and can incorporate various data parameters that it integrates into a simple visual representation in the form of a pie.[30] The data compiled from various sources such as *in vitro* assays are assimilated at the discretion of the user based on preset and post modification settings in the ToxPI GUI.[31] Each pie chart produced by ToxPI is a depiction of one specific chemical, whereas the slices that make up the pie chart are components or attributes of a chemical such as chemical properties, biological pathways, and exposure data (Figure 2). These slices in turn can be made of multiple smaller slices, which are representatives of each assay or endpoint that is used. Each slice of the pie chart for each chemical can also be given higher priority over other assays by giving more "weight" to a specific assay and less weight to a non-specific assay thus effecting the size of the pie charts.

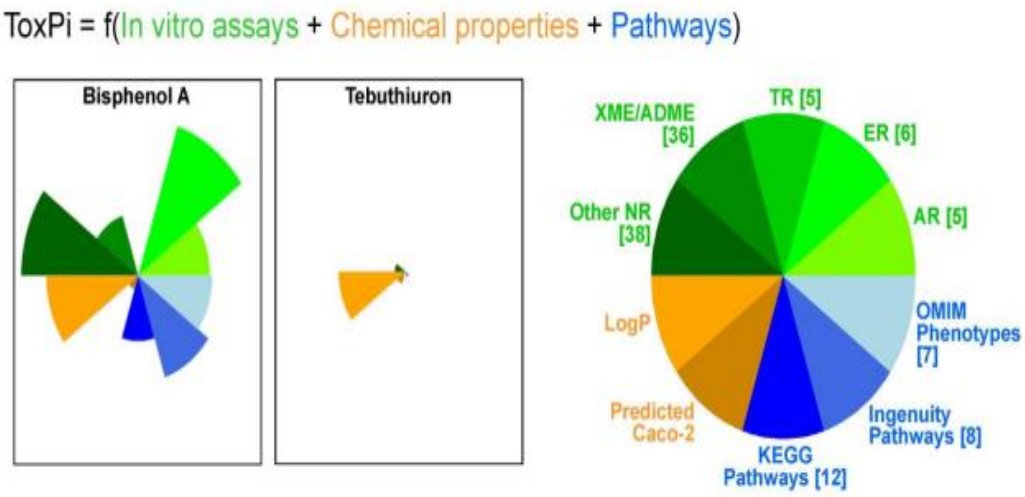

Figure 2. ToxPI Visualization Chart. ToxPI can incorporate data based off a variety of chemical's properties, bioactivity, and in vitro assay data. The various data parameters can then be compared to one another and displayed as a visual pie chart. Those chemicals with the larger pie charts have the highest predicted effects whereas the chemicals with smaller pie charts have a smaller predicted effect. Bioinformatics. 2013 Feb 1; 29(3): 402–403. Published online 2012 Nov 29. doi: 10.1093/bioinformatics/bts686

Scaling can also be applied for each slice of a pie chart. *In vitro* data in the ToxPI is given in micromolar concentration and scaling the data in log10(x)+log10(max(x)) allows lower micromolar concentrations to result in larger pie charts while higher micromolar concentrations producing smaller pie charts.[31] ToxPI scaling is versatile and includes binary, zero to one "hit" and "non-hit" systems, and linear scaling that allows smaller numbers to result in reduced pie charts and larger numbers to result in greater pie charts. Scaling each slice specifically for its data allows different slices to be compared to one another despite each slice of a chemical's pie chart representing different aspects its

attributes.

The outcome of setting these different pathways not only produces a pie chart visualization but takes in all information about a specific chemical and reduces it to a unit-less number. In other words, each slice is ranked on a dimensionless number system ranging from 0 to 1. A non-effective chemical slice would have the least effect (0) and those with the highest predicted effects would be given a 1. The total sum of every slice produces the overall ToxPI score. If a chemical in ToxPI is composed of five slices those with the greatest effects would not only be the biggest pie chart but would have the highest score (5) whereas the lowest number would be 0 and the pie chart would be unfilled.

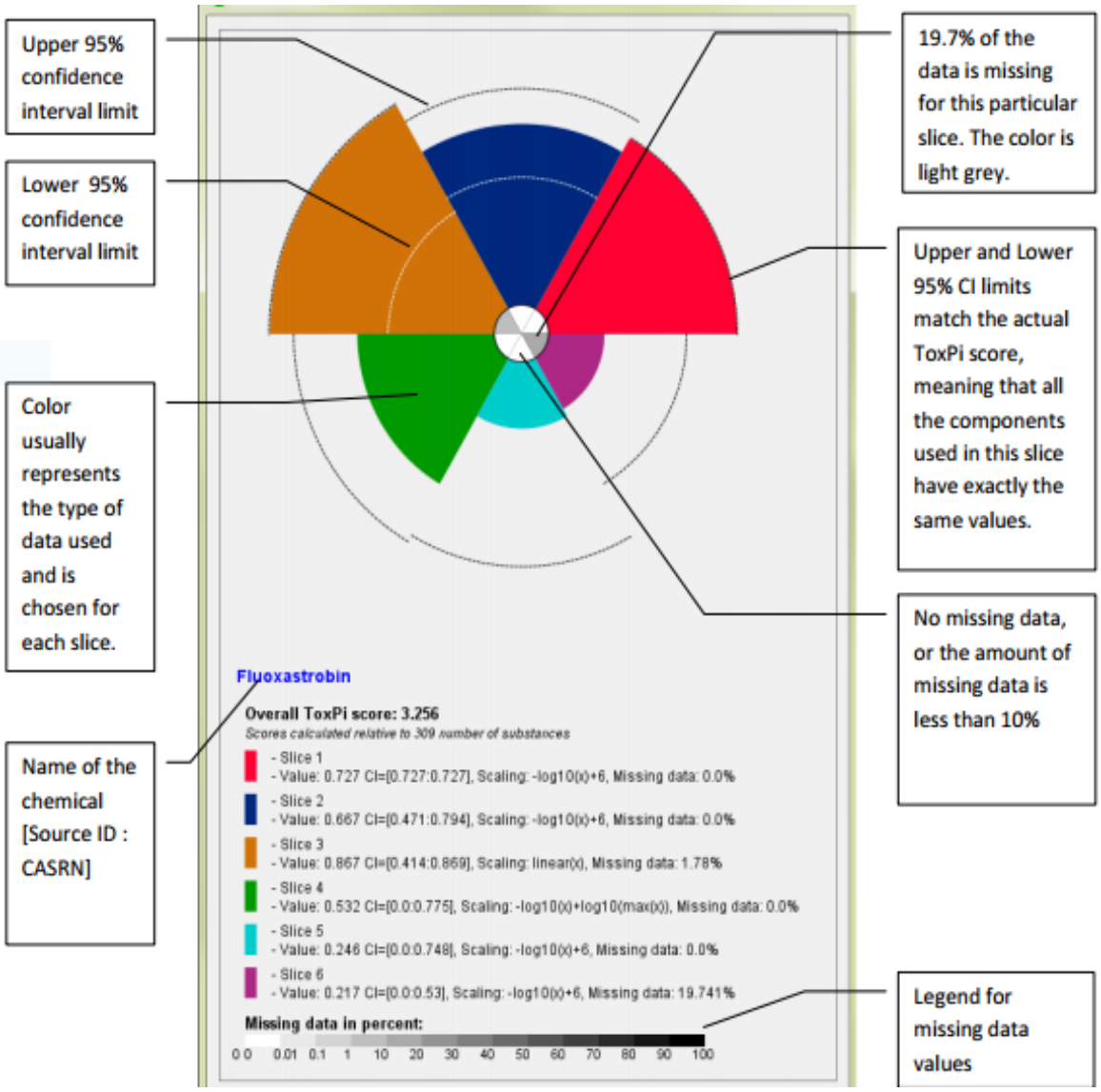

Figure 3. Window Preview of ToxPI Data. Chemicals properties are divided by an individual color and is turn made up of multiple smaller slices. For each color, appropriate scaling is applied for every data set and conference intervals are calculated. Missing data % is shown in the middle of each ToxPI and an overall ToxPI score is generated. Environ Health Perspect. 2010 Dec; 118(12): 1714–1720.Published online 2010 Sep 8. doi: 10.1289/ehp.1002180

The ToxPI GUI produces a short summary for each of the calculated chemicals. It gives vital information on the ToxPI score, its value broken up into specific slices, how many chemicals are being ranked against each other and the missing data in value percent. This value percent is also seen in the middle of each ToxPI slice (Figure 3). Those with more grey or dark shades in the middle of their ToxPI calculations have missing data. All chemicals are also visualized on the same ToxPI plane and are given in a standard X, Y graph (not shown). In this format, the standard deviations are shown between the chemicals and how these could affect the chemicals rank. Y values represent the chemical ranks whereas the X value represent the calculated ToxPI scores for each of the chemicals.

The Interactive Chemical Safety and Sustainability Database

Data for the ToxPI software can be mined using the Aggregated Computational Toxicology Online Resource (ACToR) database and can be easily exported using the interactive Chemical Safety and Sustainability (iCCS) tab. The interactive iCCS dashboard contains data from multiple database sources including Toxicity Forecaster (Toxcast) and Toxicity Testing in the 21st century (Tox21); the latter has been assimilating data since 2007. The iCCS houses data on just over 9,076 chemicals and just under 1,200 assays. The data can be filtered by different parameters such as a specific time points, specialized tissues, cell type, and gene expression.

Other information on bioactivity of chemicals are also available such as human oral absorption and LogP values. The iCCS database assays are all given in activity call (AC50) values, which are a superset of the classical known 50% inhibition of cytotoxicity and 50% inhibition of differentiation values. AC_{50} values are indicative of either inhibitory or activation effects. After filtering through selected parameters at the discretion of the user the iCCS data can then be exported via a downloadable excel workbook. The excel file then can be reformatted to fit the ToxPI system and integrated into a matrix that can be uploaded into the ToxPI program itself. ToxPI analysis has been useful in assessing the ability of novel chemicals to disrupt endocrine receptors[32], vascular development and remodeling[33], and evaluate risk associated with obesity and diabetes.[34]

Aims and Objectives

Previous data from the zur Nieden lab (see chapter 3) points to an inhibition of osteogenesis caused by various tobacco products. However, overall, it is challenging to decipher how an individual chemical in tobacco smoke contributes to toxicity or teratogenic effects during embryogenesis. A major obstacle in studying these effects is the tobacco smoke itself, a concoction composed of more than 7,000 chemical constituents. With the passage of the Family Smoking and Prevention Act the Food and Drug Administration (FDA) in 2009 released a list of harmful and potentially harmful constituents (HPHCs) in

tobacco products and tobacco smoke.[36] While most of the chemical constituents in tobacco smoke and products remain incompletely identified, the HPHC may provide a good framework for focusing on those chemicals that pose the greatest threat to human health. While the HPHC list has substantially reduced the number of chemicals to test down to 97, testing these chemical constituents individually or in assortments would be a time consuming and expensive venture. Therefore, the specific objectives of this study will address the following two specific aims.

Specific Aim 1: Use ToxPI as a prioritization tool to rank and predict chemical constituents in tobacco products that can have cytotoxic and teratogenic effect on skeletal development.

Specific Aim 2: Determine the toxicity of the highest predicted chemicals through a well-established *in vitro* osteogenic protocol using human ESCs.

CHAPTER TWO

MATERIALS AND METHODS

Materials

1. mTESR™ 1 (Stem Cell Technologies, cat. no. 85850). mTESR medium was sold as a kit that included basal medium and supplements. The medium was completed when the supplements were added to the basal medium. Stored at 2-8 °C.
2. DMEM with 4500 mg D-Glucose/L (Stem Cell Technologies, cat. no. 36250). Stored at 2-8 °C.
3. Dulbecco's Modified Eagle's Medium and Ham's F-12 Nutrient Mixture (DMEM/F12) (ThermoFisher, cat. no. 11320-033). Stored at 2-8 °C.
4. 1X Phosphate Buffered Saline (PBS) without calcium, magnesium, or phenol red, sterile, pH 7.4 (ThermoFisher, cat. no. 10010-023). Stored at 2-8 °C.
5. Human embryonic stem cells (hESC), (e.g. H9 line from WiCell Research Institute).
6. Human foreskin fibroblasts (hFF) (ATCC, cat. no. CRL-2429™).
7. 2% gelatin, sterile cell culture grade (Sigma Aldrich, cat. no. G1393) Working 0.1% Gelatin: 2 mL of a 2% gelatin stock solution to 38 mL of pre-autoclaved

sterile water. 0.1% gelatin was filtered using a 0.1 µm filter and stored at 2-8°C.

8. Dimethyl Sulfoxide (DMSO) (Sigma, cat. no. 472301). Stored at room temperature.
9. Matrigel Matrix hESC (Stem Cell Technologies, cat. no. 354277). The 5 mL vial of Matrigel matrix was thawed overnight at 2-8°C. Thawed matrigel matrix was diluted 1:1 with 5 mL of cold DMEM/F12, and completely mixed, and placed in 1 mL aliquots into 15 mL conical tubes. These aliquots were stored at -20°C until needed. Working Matrigel: 1 mL of 1:1 diluted Matrigel Matrix aliquot was thawed at 2-8°C and 14 mL of cold DMEM/F12 was added. Working Matrigel can be stored at 2-8°C
10. Accutase, pre-made in Dulbecco's phosphate-buffered saline (DPBS) without Ca^{2+} and Mg^{2+} (Innovative Cell Technologies, cat. no. AT-104). Stored at 2-8 °C.
11. Batch-tested fetal bovine serum (FBS). Stored at -20°C.
12. 100X MEM Non-Essential Amino Acid (NEAA) solution (Sigma, cat. no. RNBD8621). Stored at 2-8 °C.
13. 10,000 U/mL Pencillin/Streptomycin (Lonza, cat. no. 17-602E). Stored at 2-8 °C.
14. 2-Mercaptoethanol (*β*-ME) (Gibco, cat. no. 21985). Stored at 2-8 °C.
15. Beta-Glycerophosphate (BGP) (Sigma, cat. no. 65422). A 1 M stock was prepared by adding 10.802 grams into 50 mL of PBS and stored at -20°C.

16. 1-α, 25-$(OH)_2$ vitamin D_3 (Vitamin D_3) (Sigma Aldrich, cat. no. 17936). A stock of 50 mg/mL by adding 2.5 grams into 50 mL of PBS and stored at -20°C.
17. Ascorbic Acid (AA). (Sigma Aldrich cat. no. A4403). A stock concentration of 50 mg/mL was by adding 2.5 grams into 50 mL of PBS and stored at -20°C.
18. 3-(4,5-dimethylthiazol-2-yl)-2,5-diphenyltetrazolium bromide (MTT) (Amresco, cat. no. 0982C140). A stock of 5 mg/mL MTT in 1X PBS was prepared. The stock was sterile filtered using a 0.1 µm filter and stored at -20°C.
19. Sodium Dodecyl Sulfate (SDS) (Sigma Aldrich, cat. no. 436143). 20% SDS solution can be made by adding 20 mL of SDS and 80 mL of PBS. Stored at room temperature.
20. Isopropanol (Sigma Aldrich, cat. no. I9516). Stored at room temperature.
21. MTT Desorb: prepare MTT desorb solution containing 3.5% of 20% SDS and 96.5% isopropanol. Stored at room temperature.
22. NP-40 (abcam, cat. no. ab142227)
23. Sodium Deoxycholate (Sigma Aldrich, cat. no. D6750)
24. Radioimmunoprecipitation (RIPA) buffer. 1X PBS containing 0.1% SDS, 1% 25. NP-40 and 0.5% sodium deoxycholate. pH needs to be set to 7.2. Stored at 2-8°C
25. Ca^{2+} reagent: 0.15 mM Arsenazo III (2,2'-bisbenzene-arsonic acid, DCL Toronto). Ready-to-use reagent. Stored away from light at room

temperature.

26. Calcium Carbonate (Fisher Scientific, cat. no. C63-10). A calcium stock solution of 10 mg/mL in PBS was prepared and stored at 2-8°C.
27. Bovine Serum Albumin (BSA). Store powder at 2-8°C. A stock solution of 50 mg/mL in PBS was prepared and stored at 2-8 °C.
28. DC Protein Reagent Kit (Biorad, cat. no. 500-0111). When ready to use 1000µL of Reagent A was mixed with 25µL of Reagent S to make a new solution A'. Stored away from light at room temperature.
29. 6-well non-treated cell culture plates (NEST Biotechnology, cat no. 703011).
30. 48-well non-treated cell culture plates (Cell Star, cat. no. 677102)
31. Absorbent underpads with waterproof moisture barrier (VWR, cat. no. 82020-845) to be used as blotting paper.
32. Flat 96-well microtiter assay plates (e.g. Corning Costar).
33. Heidolph Polymax Wave Shaker (Brinkmann).
34. Refrigerated microcentrifuge, e.g. Eppendorf 5415R and 1.5 mL microcentrifuge tubes (VWR, cat. no. 87004-262).
35. ELISA plate reader with filter sets for 550-570, 650 and 750 nm, e.g. Tecan Safire 2™.

Media

1. mTESR™ 1. Stored at 2-8°C.
2. hFF medium: DMEM, 10% FBS, 1% NEAA and 0.5% of Pencillin/Streptomycin. Stored at 2-8°C.

3. Control Differentiation Media (CDM): DMEM, 10% (FBS), 1% NEAA, 0.5% of Pencillin/Streptomycin and 0.1 mM β-ME. Stored at 2-8°C.
4. Osteogenic Differentiation Media (ODM): CDM media supplemented with 10 mM BGP, 50 mg/mL AA, and 50 mg/mL of Vitamin D_3. Stored at 2-8°C.

Chemicals

1. Nicotine (Toronto Research, cat. no. sc-N0267). Nicotine's stock concentration was made by diluting 5mg in 1mL of DMEM (5,000 µg/mL). The stock concentration was filtered using 0.1 µm filters and stored at -20°C.
2. Coumarin (Santa Cruz, cat. no. sc-205637). Coumarin's stock concentrations was made by diluting 50mg in 1mL of DMSO (50,000 µg/mL). The stock concentration was stored at -20°C.
3. Catechol (Santa Cruz, cat. no. sc-215763). Catechol's stock concentration was made by diluting 50mg in 1mL of water (50,000 µg/mL). The stock concentration was filtered using 0.1 µm filters and stored at -20°C.
4. Cotinine (Toronto Research, cat. no. C725000) Cotinine's stock concentration was made by diluting 5mg in 1.5mL of DMEM (1,292 µg/mL). The stock concentration was filtered using 0.1 µm filters and stored at -20°C.
5. Benz(a)anthracene (BAA) (Santa Cruz, cat. no. sc-252409). BAA's stock concentrations was made by diluting 50mg in 1mL of DMEM (50,000 µg/mL). The stock concentration was stored at -20°C.
6. Nicotelline (Toronto Research, cat. no. N401200). Nicotelline's stock concentration was made by diluting 5mg in 5mL of DMEM (5,000 µg/mL).

The stock concentration was subsequently filtered using 0.1 µm filters and stored at -20°C.

7. Urethane (Sigma Aldrich, cat. no. U2500). Urethane's stock concentration was made by diluting 2,000mg in 6mL of DMEM (333,286 µg/mL). The stock concentration was filtered using 0.1 µm filters and stored at -20°C.
8. Quinoline (Sigma Aldrich, cat. no. 241571). Quinoline was stored at -20°C.
9. Acrylamide (Sigma Aldrich, cat. no. 23701). Acrylamide was stored at -20°C.
10. N-formylnornicotine (NFN) (Toronto Research, cat. no. F700875). NFN's stock concentration was made by diluting 10mg in 1.5mL of DMEM (6,666 µg/mL). The stock concentration was filtered using 0.1 µm filters and stored at -20°C.
11. 4-(N-Methyl-N-nitrosamino)-1-(3-pyridyl)-1-butanone (NNK) (Toronto Research Chemicals, cat. no. M325750). NNK's stock concentration was made by diluting 10mg in 1mL of DMEM (10,000 µg/mL). The stock concentration was filtered using 0.1 µm filters and stored at -20°C.
12. 4-(methylnitrosamino)-4-(3-pyridyl) butanal (NNA) (Toronto Research, cat. no. M325650). NNA's stock concentration was made by diluting 10mg in 1mL of DMEM (10,000 µg/mL). The stock concentration was filtered using 0.1 µm filters and stored at -20°C.
13. (R,S)-N-Nitrosoanatabine (NAT) (Toronto Research, cat. no. N524750). NAT's stock concentration was made by diluting 5mg in 1.5mL of DMEM (3,330 µg/mL). The stock concentration was filtered using 0.1 µm filters and

stored at -20°C.

Websites

ToxPI program was downloaded at http://comptox.unc.edu/toxpi.php. All data was found at https://actor.epa.gov/actor/home.xhtml on the Toxicity Forecaster (ToxCast) Dashboard link.

Methods

Toxicity Forecaster Data Mining

The Environmental Protection Agency's Aggregated Computational Toxicology online resource (ACToR) was accessed at https://actor.epa.gov/actor/home.xhtml on September 20, 2017. The Toxicity Forecaster (ToxCast) Dashboard link was selected and a new window appeared. The chosen 17 chemicals were individually inserted into the chemical name search bar. Chemicals were selected with the advanced search bar that prompted an additional window to appear. Under "Filter assay using" biological processes target was selected from the drop-down menu. From the on-value section five biological processes were selected from drop-down menu: Cell Death, Cell Proliferation, Cell Morphology, Oxidative Phosphorylation, and Mitochondrial Depolarization. Selected chemical's information was viewable under the chemical and assays tabs and downloaded using the Export tab at the top right corner of the browser. For each chemical the entire process was repeated with a new window browser. All downloaded data was reformatted into

a single excel csv. file for compatibility with the ToxPI GUI. The reformatted data is shown below.

Table 1. Excel File Uploaded in ToxPI.

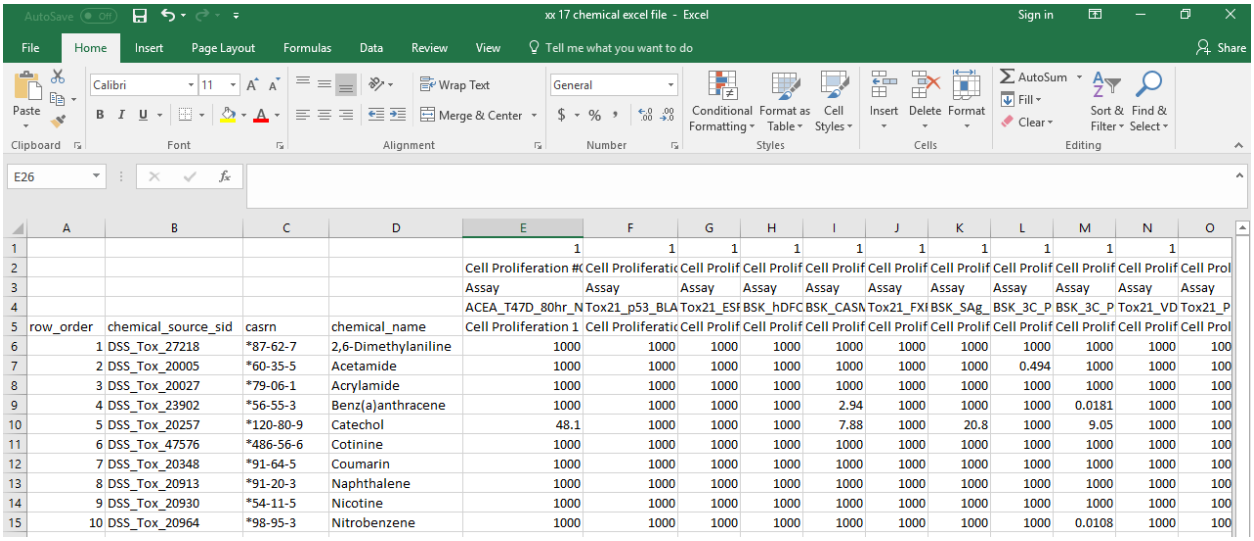

	A	B	C	D	E	F	G	H	I	J	K	L	M	N	O
1					1	1	1	1	1	1	1	1	1	1	
2					Cell Proliferation #(	Cell Proliferatic	Cell Prolif	Cell Prolif	Cell Prolif	Cell Prolif	Cell Prolif	Cell Prolif	Cell Prolif	Cell Prolif	Cell Prol
3					Assay	Assay	Assay	Assay	Assay	Assay	Assay	Assay	Assay	Assay	Assay
4					ACEA_T47D_80hr_N	Tox21_p53_BLA	Tox21_ESF	BSK_hDFC	BSK_CASN	Tox21_FXI	BSK_SAg_	BSK_3C_P	BSK_3C_P	Tox21_VD	Tox21_P
5	row_order	chemical_source_sid	casrn	chemical_name	Cell Proliferation 1	Cell Proliferatic	Cell Prolif	Cell Prolif	Cell Prolif	Cell Prolif	Cell Prolif	Cell Prolif	Cell Prolif	Cell Prolif	Cell Prol
6	1	DSS_Tox_27218	*87-62-7	2,6-Dimethylaniline	1000	1000	1000	1000	1000	1000	1000	1000	1000	1000	100
7	2	DSS_Tox_20005	*60-35-5	Acetamide	1000	1000	1000	1000	1000	1000	1000	0.494	1000	1000	100
8	3	DSS_Tox_20027	*79-06-1	Acrylamide	1000	1000	1000	1000	1000	1000	1000	1000	1000	1000	100
9	4	DSS_Tox_23902	*56-55-3	Benz(a)anthracene	1000	1000	1000	1000	2.94	1000	1000	1000	0.0181	1000	100
10	5	DSS_Tox_20257	*120-80-9	Catechol	48.1	1000	1000	1000	7.88	1000	20.8	1000	9.05	1000	100
11	6	DSS_Tox_47576	*486-56-6	Cotinine	1000	1000	1000	1000	1000	1000	1000	1000	1000	1000	100
12	7	DSS_Tox_20348	*91-64-5	Coumarin	1000	1000	1000	1000	1000	1000	1000	1000	1000	1000	100
13	8	DSS_Tox_20913	*91-20-3	Naphthalene	1000	1000	1000	1000	1000	1000	1000	1000	1000	1000	100
14	9	DSS_Tox_20930	*54-11-5	Nicotine	1000	1000	1000	1000	1000	1000	1000	1000	1000	1000	100
15	10	DSS_Tox_20964	*98-95-3	Nitrobenzene	1000	1000	1000	1000	1000	1000	1000	1000	0.0108	1000	100

ToxPI Pie Chart Generation

The ToxPI GUI was downloaded at http://comptox.unc.edu/toxpi.php and saved as a java application on the desktop. Data exported from the Toxicity Forecaster was reformatted in an excel sheet and inserted into the ToxPI program (download and format instructions above). The ToxPI GUI was opened and the reformatted excel sheet was uploaded by the insert tab. In total, seventeen chemicals were chosen manually and the generate charts icon was

selected which allowed each of the biological processes to be sorted. The data was sorted by the assays option and each assay option was named for each biological process. For each assay option a corresponding data selection icon appeared and data for each biological process was selected manually. Each biological process was given its own unique color using the color bar; Cell Morphology 2 assays (Green), Mitochondrial Depolarization 5 assays (Purple), Oxidative Phosphorylation 8 assays (Yellow), Cell Death 27 assays (Black), and Cell Proliferation 30 assays (Red).The 5 biological processes pie slices were given scaling via scaling option by selecting -log10(x)+log10(max(x)) on the drop-down menu, this would ensure that lower active AC50 values were given separation from non-active hits. Pie charts were generated by selecting final generation tab and individualized pie charts were displayed on the screen. Pie charts for all 17 chemicals were saved by selecting save images option. The ToxPI images were saved individually and together.

Cell Passaging and Maintenance

hFF Culture Maintenance. hFFs were obtained from ATCC and were grown in 0.1% gelatin pre-coated 6-well plates and kept at 37°C in a controlled humidified 5% CO_2 incubator. 6-well plates were pre-treated with 0.1% gelatin for 15 minutes before the start of passaging and subsequently removed. While in culture hFFs were routinely checked for bacterial, yeast, and microbial contamination using an inverted microscope. Cultures were also checked via the inverted microscope for confluency. Cultures were considered confluent when

hFFs covered 70% of the surface area of an individual 6-well and were passaged in a 1:6 ratio. When a 6-well culture reached confluency hFF media was removed and washed with PBS. PBS was subsequently removed and treated with 1mL of Accutase. When hFFs dissociated and were suspended in solution, 1mL of hFF media was added and consequently put in a 15mL conical tube and spun down in a microcentrifuge. The supernatant was removed, and the left-over pellet was resuspended in 6mL of hFF media. Each well of a 6-well plate was given 1mL of the resuspended hFF cell suspension. hFFs were passaged every two to four days when cells reached 70% confluency.

Human Embryonic Stem Cell Culture Maintenance. H9 hESCs were obtained from WiCell. All human pluripotent cells were maintained in mTESR media in pre-treated matrigel coated 6-well plates. 6-well plates were coated with matrigel for 20-30 minutes and subsequently removed prior to the start of passaging. hESCs were grown in an incubator at 37°C in a controlled 5% CO_2 humidified incubator. While in culture cells were routinely checked for bacterial, yeast, and microbial contamination using an inverted microscope. Cell morphology was also assessed during this time to ensure pluripotency of the H9 cells. Cells that began to differentiate (fissured morphology) were discarded and new H9s were used. 6-well cultures were assessed for confluency with an inverted microscope and passaged when colonies covered 70% of the surface area of an individual 6-well plate. Cells were also passaged when colonies grew close to each other but were not touching. Cultures that reached confluency were

passaged in a 1:6 ratio. Confluent culture's mTESR media was removed and washed with PBS. The PBS was removed, and cells were treated with 1mL of Accutase. When colonies dissociated and were suspended in Accutase, 1mL of mTESR was added and consequently put in a 15mL conical tube and spun down in a microcentrifuge. The supernatant was removed and resuspended in 6mL of mTESR. Each well of a 6-well plate was given 1mL of the resuspended cells in mTESR. hESCs were passaged every two to four days as needed.

Cell Counting and Seeding. Seeding density was calculated from a 6-well plate to a 48-well plate for the MTT and calcium endpoints. The surface area ratio was calculated by dividing the area of 6-well plate over the surface area of a 48-well plate. The surface area ratio was multiplied by the passage ratio 1:6 to obtain the dilution factor. The resuspended cell volume was divided over the dilution factor and multiplied by 1000 to obtain the appropriate amount of cell suspension needed per well of a 48-well plate. The cell suspension needed per an individual 48-well was multiplied by the number of wells needed for the total cell suspension. The total volume of media was calculated by the amount of media (300µL) per individual 48-well multiplied by the number of wells. The total cell suspension and total volume of media were mixed and 300µL was added to each 48-well plate.

Osteogenic Differentiation and Endpoints

H9 hESCs were seeded into 48-well plates from a 6-well plate (Cell counting and seeding instructions above). Cells were grown to 70% confluency

and checked daily using the inverted microscope. When cells reached 70% confluency or when colonies grew close to one another without touching the differentiation protocol was started. mTESR medium was removed from each of the wells and replaced with CDM. hESCs were given CDM until Day 5 where the media was removed and replaced with ODM. Cells continued to grow in ODM until Day 20. Media was replaced every 2-3 days during the differentiation experiment.

Dilution Series. Cells from Day 0 to Day 20 were fed with a specific starting concentration for each chemical, starting from the stock, each concentration was made by subsequent serial dilutions (all chemicals tested were in a 10-fold dilution series).

MTT Assay (Cell Viability). To determine cell viability hESCs and hFFs were seeded (Cell counting and seeding instructions above) in separate 48-well plates with 5 replicates for each test chemical concentration. hESCs were differentiated into osteoblasts using our labs osteogenic protocol while hFFs were fed hFF media during the entirety of the experiment. On day 20 cells were supplemented with 50µL of PBS dissolved MTT for each well containing 300µL of medium and placed inside an incubator for 2 hours in 5% CO_2 atmosphere at 37°C under sterile conditions. After the 2-hour incubation period the 48-well plates were placed upside down on blotting paper where the media was absorbed and discarded. 325µL of MTT Desorb was added to each of the 48-wells and placed on a micro-shaker for 15 minutes. 100µL of each well with MTT

desorb was pipetted into a 96-well plate and the absorbance was read at 570nm with a Bio-rad iMark™ microplate reader. The percent cell viability was calculated by normalizing treated wells with non-treated control wells.

Lowry Assay (Protein Determination). To determine protein content, hESCs were seeded (Cell counting and seeding instructions above) in a 48-well plate with 5 replicates for each test chemical concentration and differentiated into osteoblasts using our labs osteogenic protocol. Upon collection (Day 20) CDM media was removed and hESCs were washed with PBS. After the removal of PBS, 300µL of RIPA buffer was added to each well and scrapped using a pipet tip to dislodge the calcium from the base of the culture vessel. The scrapped RIPA lysates were collected and placed into Eppendorf tubes. Protein standards were prepared from the BSA stock solution in a 7 concentration serial dilution series that ranged from 0.0 mg/mL – 1.5 mg/mL. 5µL of each BSA standard concentration and RIPA collected lysates were placed into a 96-well plate. Approximately 25µL of Reagent A' was combined with RIPA lysates and BSA concentrations and 200µL of Reagent B was subsequently added. The 96-well plate was incubated for 15 minutes on a micro-shaker and absorbance was read at 750nm on a Bio-rad iMark™ microplate reader. Protein concentration was determined by standardizing each well to the BSA protein concentration curve. The curve was developed by graphing absorbance as the x-axis and the BSA standard concentrations as the y-axis. A linear regression line was drawn with y = m × x, where y= protein concentration in mg/mL, m = slope and x =

absorbance. The mean blank was subtracted from all sample values and the total protein content was calculated by multiplying the volume of the sample (0.3mL) by the protein concentration in mg/mL.

Calcium Determination. The calcium assay was performed with the same RIPA collected samples from the Lowry assay. A standard curve was developed from the 10 mg/mL calcium stock solution for 8 concentrations in serial dilution that ranged from 0.0 - 0.03 mg/mL Ca^{2+}. 25µL of each calcium standard curve concentration and RIPA collected lysates were placed into a 96-well plate. Additionally, 75µL of Arsenazo III was added to each 96-well plate and absorbance was read at 655nm with a Bio-rad iMark™ microplate reader. The calcium standard curve was drawn based off the values of the calcium standard concentrations as the y-axis and absorbance as the x-axis. A linear regression line ($y = m \times x$) was drawn through 0 intercept where the slope was m, absorbance as the x, and calcium concentrations in mg/mL as the y. The blank value was subtracted from the sample values and total calcium content of each sample was calculated by the volume of the sample multiplied (0.3mL) by the calcium concentration in mg/mL. The total calcium content was normalized to the total protein content that was measured with the Lowry assay. The untreated wells were averaged and set to 100 percent and all values were calculated as percentage of the untreated average. The mean and the standard deviation for all test chemical concentrations were also calculated. The data was graphed with the x-axis as the test chemical concentrations from low to high (left to right) and

the y-axis as the percentage.

Classification of Tested Chemicals in the EST Biostatistical Model

The embryotoxic potential of the test chemical was calculated from the IC_{50} and ID_{50} values. The IC_{50} and ID_{50} values were determined by graphical estimation. The ID_{50} for the differentiation endpoint (hESCs) was put into relation to the cytotoxicity endpoints (IC_{50} hESC and IC_{50} hFF) by insertion into three linear discriminant functions.

I: $$5.9157\ \log_{10}(IC_{50\ hFF}) + 3.500\ \log_{10}(IC_{50\ hESC}) - 5.307\frac{IC_{hFF} - ID_{50\ hESC}}{IC_{50\ hESC}} - 15.72$$

II: $$3.651\ \log_{10}(IC_{50\ hFF}) + 2.394\ \log_{10}(IC_{50\ hESC}) - 2.033\frac{IC_{hFF} - ID_{50\ hESC}}{IC_{50\ hESC}} - 6.85$$

III: $$-0.125\ \log_{10}(IC_{50\ hFF}) - 1.917\ \log_{10}(IC_{50\ hESC}) + 1.500\frac{IC_{hFF} - ID_{50\ hESC}}{IC_{50\ hESC}} - 2.67$$

A chemical was classified as non-embryotoxic agent when values determined I>II and I>III (class I), as a weak embryotoxic agent (class II) if II>I and II>III, and a strong embryotoxic agent (class III) when III>I and III>II.

CHAPTER THREE

PREVIOUS DATA

Osteogenic Protocol

Human ESCs were grown on matrigel coated plates and fed with mTESR until they reached 70% confluency. Upon reaching confluency the media was replaced with control differentiation media largely composed of Fetal Bovine Serum (FBS) and Basal Medium Eagle Medium (DMEM). Cells were grown in control differentiation media until day 5 when the medium was supplemented with osteogenic factors 1-alpha,25 $(OH)_2$ (Vitamin D3), ascorbic acid (AA), and beta-glycerophosphate (BGP) (Figure 4A).

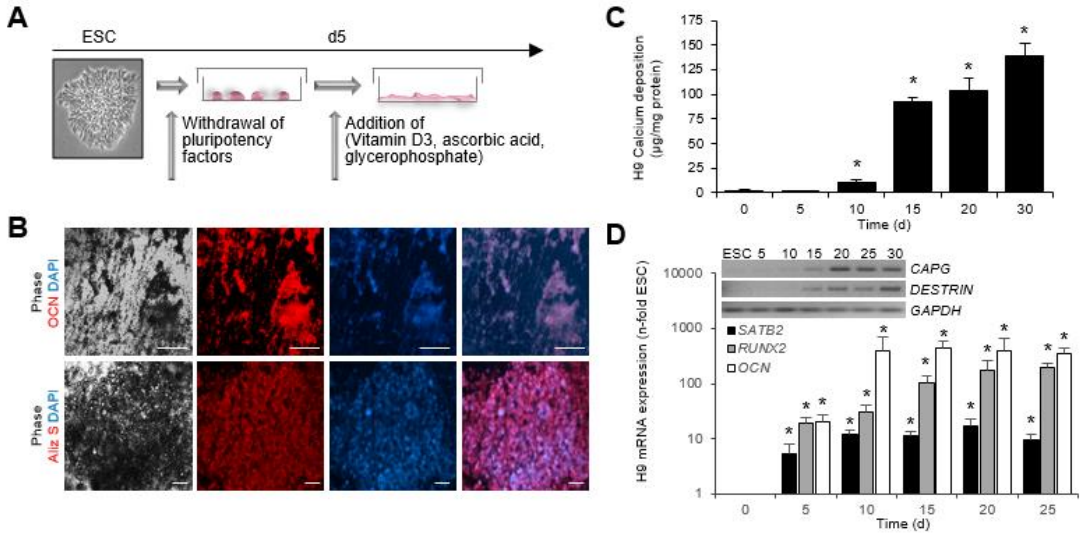

Figure 4. Determination of Osteogenic Differentiation and Identity. (A) Schematic of the osteogenic differentiation protocol. (B) Immunostaining with an osteocalcin antibody reveals presence of bone matrix in the vicinity of black deposits. Alizarin Red S staining detected calcium ions in the same areas. (C) Quantitative measurement of deposited calcium over time, n=5 independent replicates ± SD, **P*<0.05 Student's t test compared to d0. (D) Quantitative mRNA analysis of *RUNX2, SATB2* and *OCN*, normalized to *GAPDH* (n=3 independent samples ± SD), **P*<0.05 One-Way ANOVA over day 0. Triplicates were pooled for RT-PCR analyses of the osteocyte genes *CAPG* and *DESTRIN* (inset). Unpublished data.

Osteocalcin, a protein that is secreted by osteoblasts into the extracellular matrix of bone was identified in cultures. Likewise, Alizarin Red S further confirmed the calcification of the ECM another hallmark as the result of osteoblast formation (Figure 4B). Calcium deposition were shown to increase throughout 30 days of the osteogenic differentiation (Figure 4C). Quantitative mRNA confirmed the presence of *RUNX2*, an early osteogenic marker that controls other osteogenic markers, *SATB2* an osteogenic progenitor marker, and *OCN* a mature osteoblast marker (Figure 4D). CapG and Destrin presence are indicative that osteoblasts are maturing into osteocytes.

Tobacco Exposure and Osteogenesis

The lab next tested the effects of tobacco on osteogenic differentiation. Among the tested products were two conventional cigarettes, one additive-free variety and two so-called ‘Light’ cigarettes. Both mainstream (MS) smoke, which is what the smoker inhales, and side-stream (SS) smoke, which burns off the tip of the cigarette, were tested. The conventional products caused no significant change in cell viability or calcification for any of the tested concentrations (Figure 5A). In contrast, the conventional side stream smoke showed a decrease in cell viability and calcification, with both curves overlapping (Figure 5B), suggesting that the differentiation defect was caused by the cytotoxicity of the product.

While the additive-free cigarette smoke extract behaved similarly as the conventional products did, the two harm-reduction cigarettes exhibited very different patterns. Harm-reduction SS smoke caused a significant decrease in calcification already at sub-toxic concentrations (Figure 5D). This poses a significant issue for *in utero* exposures since it implies that surviving cells are defective potentially resulting in developmental abnormalities for the fetus during pregnancy. This truly teratogenic effect was seen also in MS smoke of the harm-reduction brands, albeit at high concentrations. These results let us conclude that harm-reduction cigarettes may be more detrimental to the developing fetus than conventional cigarettes.

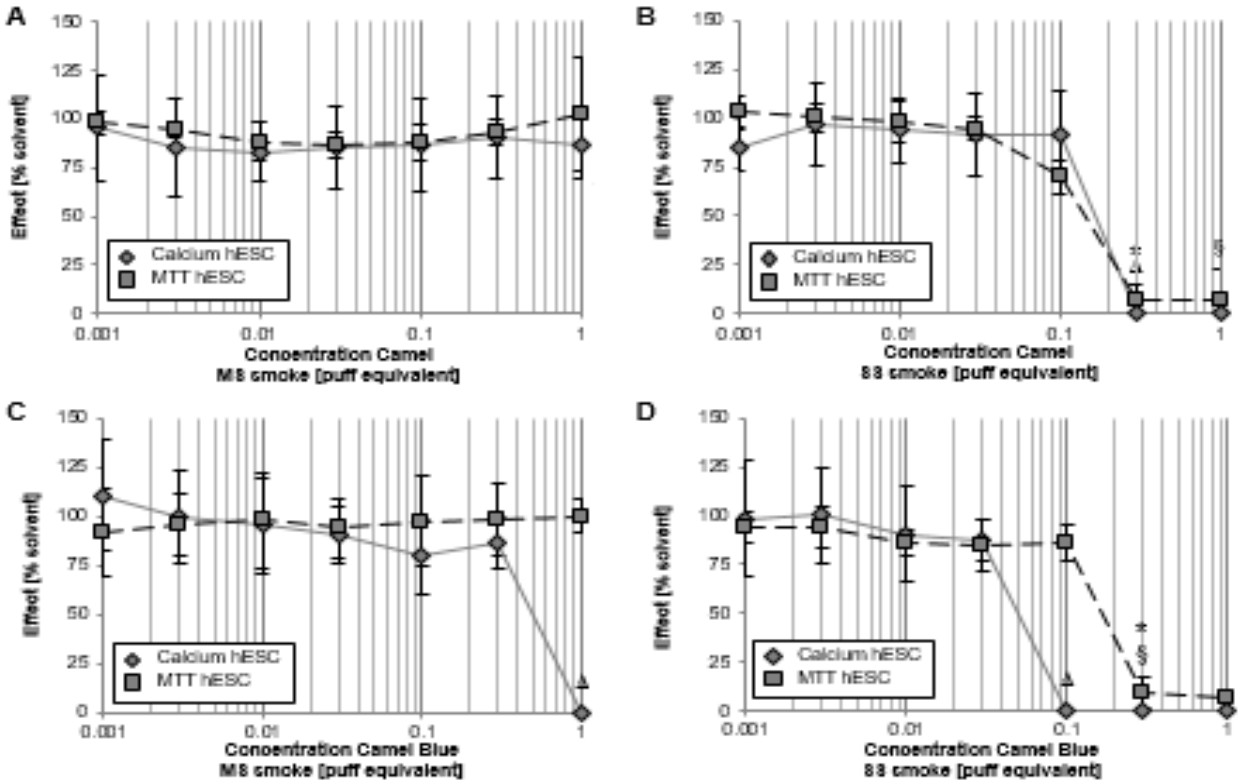

Figure 5. Determining Osteogenic Toxicity in Conventional and Light Camel Cigarettes. Human ESCs were treated with different concentrations of MS smoke solution and scored for effects on calcium deposit using Arsenazo III and on viability using an MTT assay. A) Camel MS smoke solution. B) Camel SS smoke solution. C) Camel Blue MS smoke solution. D) Camel Blue SS smoke solution. Each data point is the mean of three independent experiments ± standard deviation. $^{\Delta}P<0.05$ = lowest concentration significantly below the untreated control in the calcium assay determined by One-Way ANOVA. $^{*}P<0.05$ = lowest concentration significantly below the untreated control in the MTT assay on H9 hESCs determined by One-Way ANOVA. hESC, human embryonic stem cell; MS, mainstream; MTT, mitochondrial dehydrogenase activity assay; SS, side-stream. Unpublished data.

CHAPTER FOUR

RESULTS

ToxPI Development and Production

Of the 93 chemicals on the FDA's tobacco products and smoke HPHC list only 46 were found in the Toxicity Forecaster database. With the intention of making ToxPI parameters specific to osteogenesis a variety of genes necessary for bone development were examined in the Toxicity Forecaster. Genes such as *Frzzld*, *CatB*, and *FoxO* paramount to osteogenesis were incomplete for each of the remaining 46 tobacco constituents. Using incomplete data sets introduced large margins of errors in the ToxPI prediction model and were not useful for meaningful analysis. Other chemical properties such as oral absorption was absent for the targeted chemicals. To use ToxPI as a useful prioritization tool it was then decided to use biological processes as the driving data parameter. This shortened our remaining HPHC list of 46 chemicals to 17. Biological processes are normal functions that all cells must undergo to be viable. Though these parameters are broad and not osteogenically specific, their inclusion would be appropriate as any perturbations of these biological processes could alter cell fate and differentiation capabilities of hESCs.[24]

Furthermore, additional parameters were implemented. Row 1 data on the reformatted excel sheet was given a value of 1 to ensure equal weight among assays and biological processes. Each assay was also renamed in Row 5 to its

corresponding biological process. To predict long term exposure 24, 48, and 72-hour assays were used where shorter duration assays were disregarded. All assays were further optimized to include human cell lines for a variety of tissues and non-human animal data was excluded to avoid species-to-species differences in chemical sensitivities. Each biological process was given its own unique color (Figure 6) and scaling was applied to each of data sets to ensure that lower AC_{50} values were indicative of bigger pie charts where larger values produced smaller visualizations. Out of the 17 ToxPI predictive pie charts 8 chemicals generated ToxPI positive results where 9 of the chemicals did not produce a visualization (Figure 7).

Biological Process	**Data Type**	**Weight**	**Components**
Cell Proliferation (Red)	Assay	1	30
Cell Death (Black)	Assay	1	27
Oxidative Phosphorylation (Yellow)	Assay	1	8
Mitochondrial Depolarization (Purple)	Assay	1	5
Cell Morphology (Green)	Assay	1	2

Figure 6. ToxPI Integrated Components. Each biological process was given its own pie chart slice (5) based off assay data and had equal weight. In total, 72 assays encompassed all five biological process slices. Each slice was then given its own color; Cell Proliferation (Red), Cell Death (Black), Oxidative Phosphorylation (Yellow), Mitochondrial Depolarization (Purple), and Cell Morphology (Green).

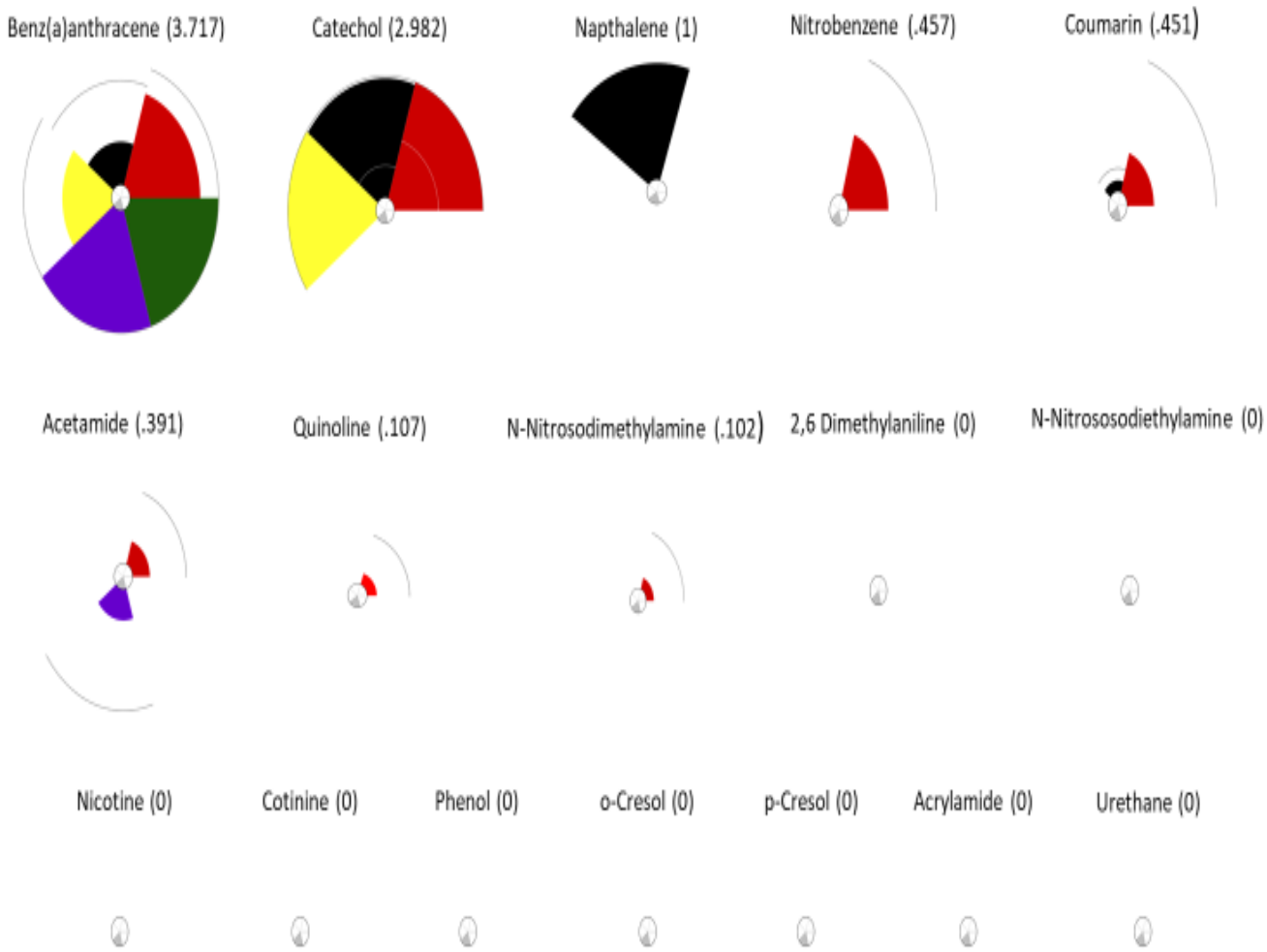

Figure 7. ToxPI Generated Charts**.** ToxPI charts were generated for 17 chemicals using 72 *in vitro* assays across 5 biological processes. Benz(a)anthracene (3.251), Benzo(b)fluoranthene (2.137), Catechol (2.15), Napthalene (1), Nitrobenzene (.457), Coumarin (.451), Acetamide (.391), Quinoline (.107), and N-Nitrosodimethylamine (.102) had designated “hits” and produced positive ToxPi values (0< X). The remainder of the chemicals 2,6 Dimethylaniline, Acrylamide, Nitrososodiethylamine, Nicotine, Cotinine, Phenol, o-cresol, p-cresol, and Urethane had ToxPI predicted null effects (X=0).

To compare the predicted value assigned to each chemical using ToxPI with its actual cytotoxicity and skeletal toxicity, we next chose a set of chemicals

to test *in vitro* using the human EST that the lab had established previously. We chose these chemicals at random from ToxPI positive and ToxPI negative chemicals. The randomly selected ToxPI positive chemicals were BAA with the highest ToxPI predictive score of 3.717, catechol with the second highest score of 2.982, coumarin, which received the fourth highest score of 0.451, and quinolone, whose penultimate ToxPI positive score value was 0.107. The randomly selected ToxPI null chemicals were nicotine (0), cotinine (0), acrylamide (0), and urethane (0) (Figure 7).

Human EST In Vitro Data for ToxPI Positive Chemicals

BAA and Catechol's hFF cell line did not exhibit a loss in cell viability in the same range as their H9 counterparts (Figure 8). Quinoline's hFF cell viability was reduced at concentrations a hundred-fold higher than their H9 counterparts whereas coumarin's hFF cell viability was reduced within the same range as its H9 immature cell line. All four ToxPI constituents showed dose response curves of H9 cell viability and calcification following similar trends, it is believed that the decrease in calcification is an attributed consequence of the overall reduction in viable cells. BAA was calculated to have a 200 μg/mL H9 hESC ID_{50}/IC_{50}, catechol's H9 hESC ID_{50}/IC_{50} was 0.1 μg/mL, coumarin received a H9 hESC ID_{50}/IC_{50} of 20 *u*g/mL, and quinoline's H9 hESC ID_{50}/IC_{50} was 5.5 μg/mL. (Figure 8). All tested ToxPi charts were able to predict immature H9 cytotoxicity, though the potency of the compound could not have been assessed by looking at the

size of each predicted pie chart.

When assessing the average assay hit rate for each of the ToxPI tested chemicals, the ToxPI score and size for each pie chart varied between chemicals as did the average micromolar concentration for each chemical constituent. This discrepancy became less apparent when the assay hit rate was converted from micromolar into micrograms per microliter (Figure 9). Interestingly, the predictive value of each assay hit rate in µg/mL was relatively close to our *in vitro* H9 hESC ID_{50}/IC_{50} (Figure 9).

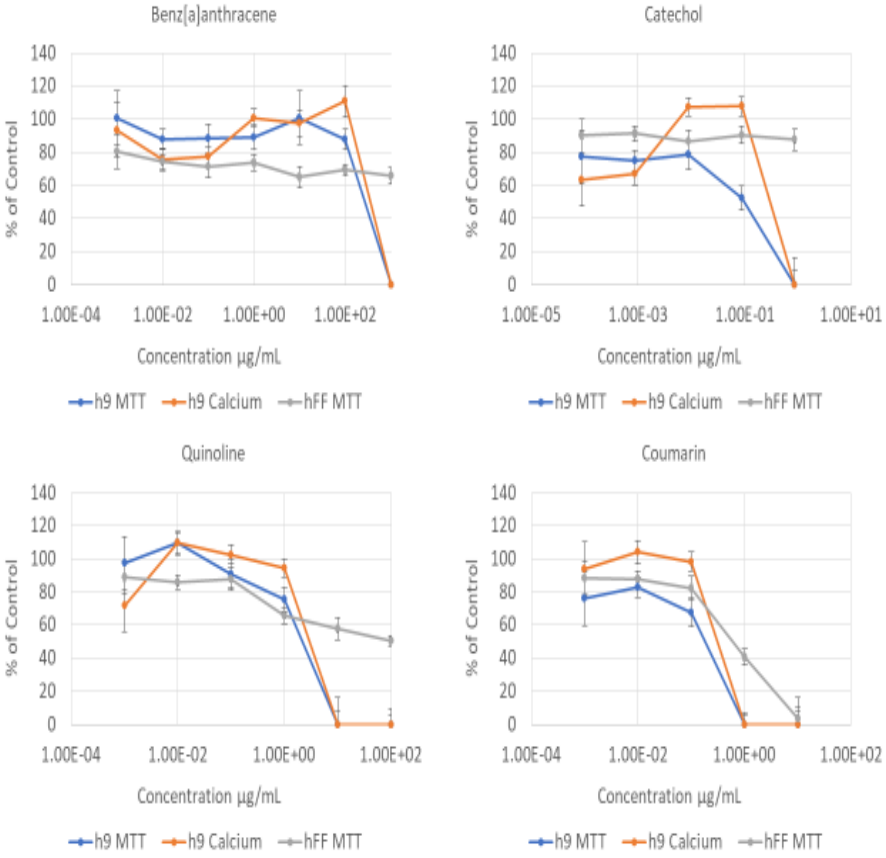

Figure 8. Determination of Skeletal Teratogenicity for ToxPI Positive Chemicals. Dose response curves for ToxPI positive Benz(a)anthracene, Catechol, Coumarin, and Quinoline. The three endpoints for the osteogenic EST; Cell Viability (MTT) of H9 hESC and hFF, and differentiation potential via assessment of calcium deposits are shown.

	BAA	Coumarin	Catechol	Quinoline
AC_{50} hit µM Average	47.04	62.51	14.70	67.80
AC_{50} hit µg/mL Average	10.73	9.86	1.16	8.76
H9 hESC ID_{50}/IC_{50} µg/mL	200 ± 76	20 ± 10	0.01 ± .005	2 ± 1.5

Figure 9. Toxicity Forecast Data Averages and In Vitro H9 hESC ID_{50}/IC_{50} µg/mL Values. The average assay hit value in µM (AC_{50}) values for each tested ToxPI positive constituent obtained from the Toxicity Forecaster database. The AC_{50} in µM for was then converted into µg/mL in comparison to the H9 hESC ID_{50}/IC_{50} values calculated from the *in vitro* osteogenic screen.

Human EST In Vitro Data for ToxPI Negative Chemicals

Four ToxPI null chemicals (nicotine, cotinine, urethane, and acrylamide) were also taken through the osteogenic EST (Figure X). ToxPI predicted null effects matched *in vitro* screen data as urethane, cotinine, nicotine, and acrylamide exposure did not inhibit cell viability for either the H9 and hFF cell lines for all tested concentration ranges (Figure 10). Likewise, H9 hESC differentiation potential was not altered in the same concentration range for urethane, cotinine, and acrylamide. However, a notable decrease in calcification (Figure 10) was seen in the higher concentrations of nicotine exposure.

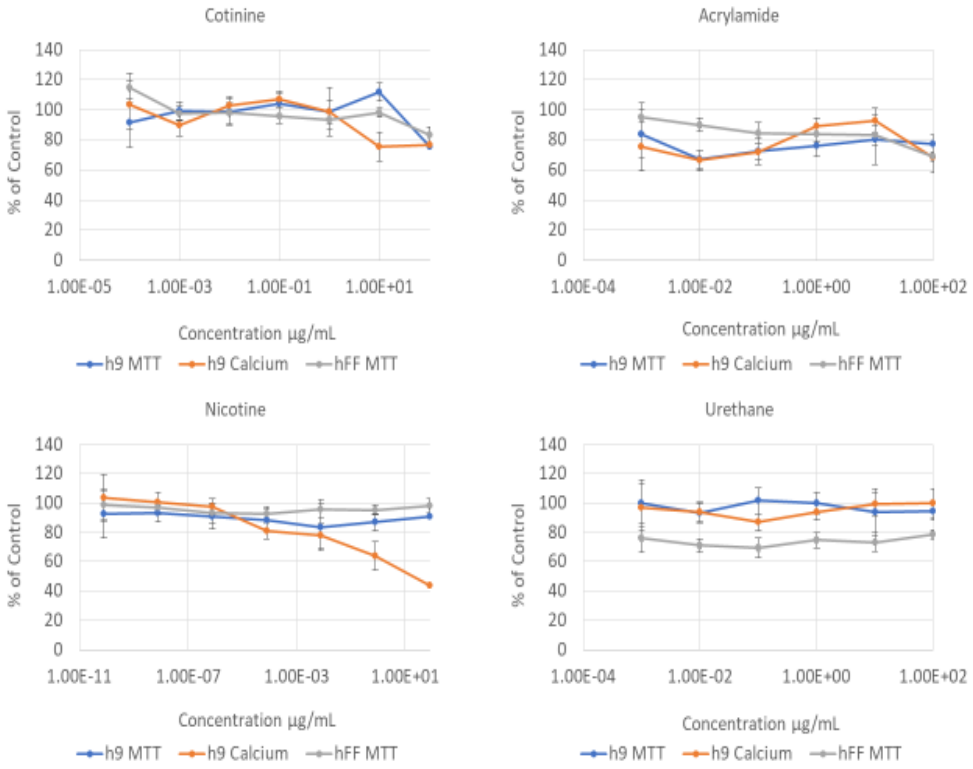

Figure 10. Determination of Skeletal Teratogenicity for ToxPI Null Chemicals. Dose response curves for ToxPI null Nicotine, Cotinine, Acrylamide, and Urethane. The three endpoints for the osteogenic EST; Cell Viability (MTT) of H9 hESC and hFF, and differentiation potential via assessment of calcium deposits are shown.

Toxicity Predictions Based on the EST Biostatistical Model

All tested chemicals hFF IC_{50} and H9 hESC ID_{50}/IC_{50} values were incorporated into the EST bio-statistical model as outlined in classification of tested chemicals in the EST Bio-Statistical Model. All *in vitro* tested ToxPI positive pie charts were classified as weakly or strongly embryotoxic, whereas all *in vitro* tested ToxPI null predicted chemicals were classified as non-embryotoxic. Coumarin and BAA were classified as weakly embryotoxic where catechol and

quinoline received a strongly embryotoxic compound status (Figure 11). The discrepancy between strongly and weakly embryotoxic seemed to have been attributed to the IC_{50} value found for the cell viability in fully differentiated hFFs in relation to those found with the undifferentiated H9 cell line.

Chemical Name	ToxPI Prediction	hFF (IC_{50}) Cytotoxicity	hESC (IC_{50}) Cytotoxicity	hESC (ID_{50}) Differentiation	EST Classification
BAA	+	—	200 ± 76	200 ± 76	Weakly Embryotoxic
Catechol	+	—	0.1 ± 0.05	0.1 ± 0.05	Strongly Embryotoxic
Coumarin	+	65 ± 26	20 ± 10	20 ± 10	Weakly Embryotoxic
Nicotine	-	—	—	0.32 ± 3	Non-Embryotoxic
Cotinine	-	—	—	—	Non-Embryotoxic
Urethane	-	—	—	—	Non-Embryotoxic
Quinoline	+	100 ± 85	2 ± 1.5	2 ± 1.5	Strongly Embryotoxic
Acrylamide	-	—	—	—	Non-Embryotoxic

Figure 11. Toxicity Classification in the EST Biostatistical Model. ToxPI predictions are listed along H9 and hFF cell viability in addition to differential potential of H9 hESCs into osteoblasts. The following ID_{50} and IC_{50} were incorporated into a bio-statistical model and classified as either Non-Embryotoxic, Weakly Embryotoxic, or Strongly Embryotoxic.

Third Hand Smoke Constituents

Third hand smoke (THS) constituents are the residue and particulate matter that persists long after a cigarette has been ignited. THS lifespan can range from several weeks to months and because of its interaction with the

environment can be more volatile as it ages. THS remain an understudied component of tobacco products and many of the chemical constituents in the HPHC largely list mainstream and side stream components. We found it of great importance to study the individual constituents that make up THS through our EST osteogenic protocol. The chemicals that were selected have been shown to persist in carpet after several months.[37] In addition, these selected THS constituents are on the FDA's HPHC list and makes them prime candidates to be tested. These constituents however were not included in the ToxPI analysis due to a lack of sufficient assay availability in the Toxicity Forecaster database.

Nicotelline's H9 hESC cell viability decreased in a similar trend with calcification, this similarity in dose response curves is likely a consequence from reduction of viable cells. Thus, an h9 hESC IC_{50} of >200 µg/mL was estimated. The adult line also decreased in the same concentration range and produced an hFF IC_{50} of >200 µg/mL. NFN, NAT, and NNK did not display cytotoxicity in the adult hFF or immature H9 cell line (Figure 12). Differentiation potential into osteoblast was also not inhibited in the same concentrations range for the tested chemicals. Though the hFF cell viability remained inert for NNA through all concentrations, a significant reduction in H9 cell viability and calcification was seen at the highest tested concentration of (4.8×10^{-4} µg/mL) (Figure 12). When grouped in ternary combination THS constituents Nicotelline, NNA, and NNK cell viability and calcification was further reduced than each chemical constituent could induce individually (Figure 13).

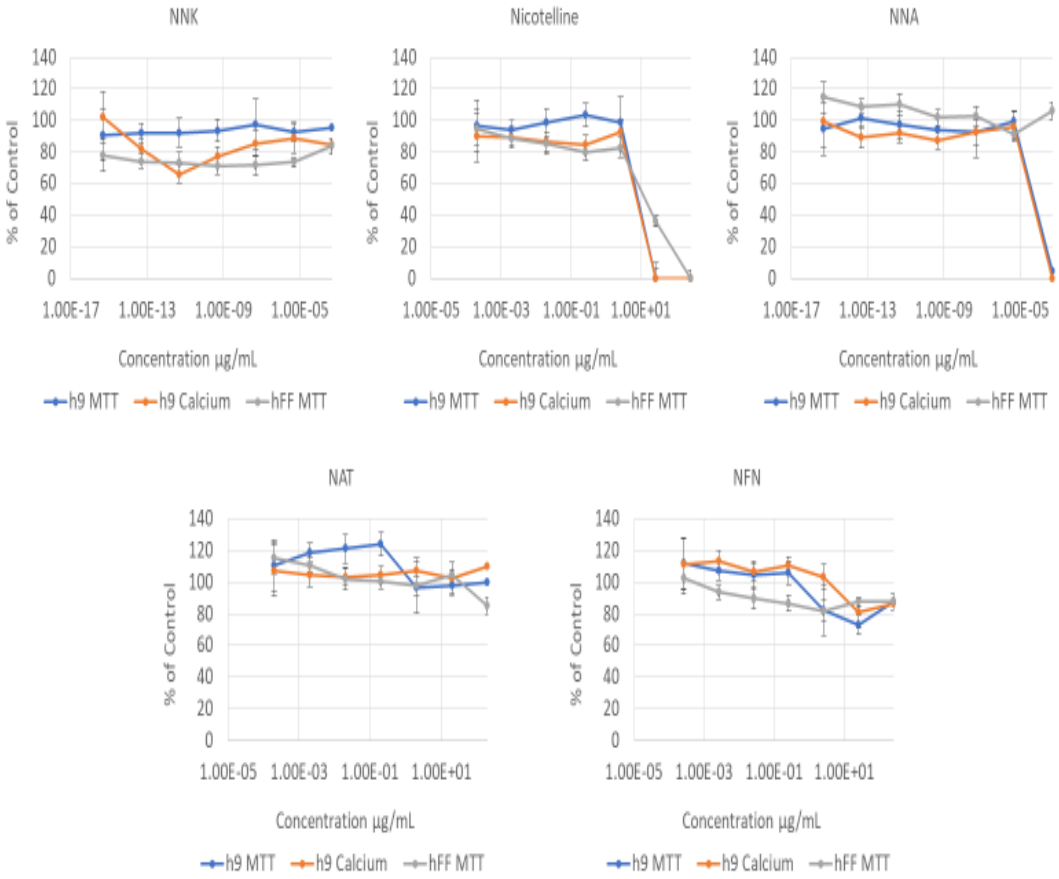

Figure 12. Determination of Skeletal Teratogenicity for Third Hand Smoke Constituents. Dose response curves for THS constituents Nicotelline, (R,S)-N-Nitrosoanatabine (NAT), N-Formylnornicotine (NFN), 4-(methylnitrosamino)-4-(3-pyridyl) butanal (NNA), and 4-(N-Methyl-N-nitrosamino)-1-(3-pyridyl)-1-butanone (NNK). The three endpoints for the osteogenic EST; Cell Viability (MTT) of H9 hESC and hFF, and differentiation potential via assessment of calcium deposits are shown.

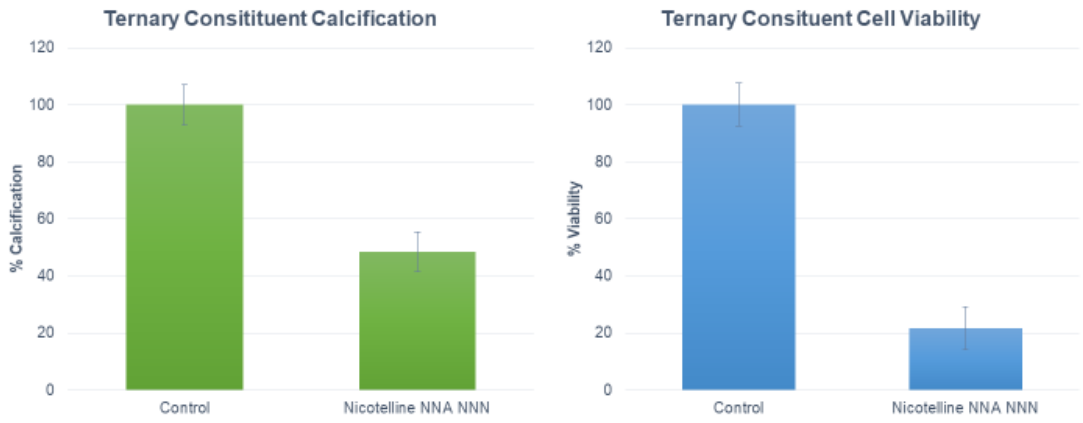

Figure 13. Cell Viability and Calcification of a Ternary Combination of THS Constituents. Three THS constituents; Nicotelline, NNA, and NNN were subjected in tandem to our osteogenic protocol. H9 hESC cell viability (MTT) and differentiation potential via assessment of calcium deposits are shown.

CHAPTER FIVE

DISCUSSION

ToxPI Predictions and In Vitro Data

Toxcast iCCS has over 11,000 chemicals and 21,000 assays available, though there was a lack of endpoints and gene targets relating to osteogenesis available in the online database. We decided to use biological processes to help predict cytotoxicity as the partition between cytotoxicity and teratogenicity is indistinguishable *in vivo*.[24] Other factors were thought to be included in addition to using biological processes' AC_{50} values (Assay hit rate) but incorporating LogP values[38] and Z-scores[39] may have not corrected potential false negatives and have been shown to remove pie charts that reflected true positives in ToxPI predictions.

The selected data used from Toxcast across the 72 assays and 5 biological processes were heavily geared towards cytotoxicity. This is due to 52 of the 72 biological processes' assays exclusively measuring cell proliferation or cell death. The assays excluded non-human cell types and multitude of cell lineages ranging from Human Embryonic Kidney (HEK) cells to umbilical vein endothelium. With this range in cell types it was likely that the H9 hESC IC_{50} values that were obtained in our *in vitro* screen would fall in the range of AC_{50} values that were available in the Toxcast. In addition to cell types, the chosen assay time endpoint excluded more short-term assays such as a one-hour

exposure time to focus on potential cytotoxic and teratogenic effect that are part of long-term exposure. The assays tested range from 0 µM to 1000 µM. The maximum threshold of 1000 µM to micrograms per milliliter can be readily converted by looking at a chemical's molecular weight. The eight tested chemicals max threshold ranged from 60 µg/mL to 228 µg/mL. Without consideration for max thresholds ToxPI predicted null pie charts could seemingly provide false negatives for chemicals whose cytotoxic and teratogenic effects are induced above the predictive threshold.

Acrylamide's ToxPI null prediction were for concentrations up to 71 µg/mL where cytotoxic and differentiation inhibition was seen at concentrations greater than 100 µg/mL (data not shown). Likewise, urethane's ToxPI null predicted chart were for concentrations up to 89 µg/mL where cytotoxic effects were seen at extreme exposure concentrations (1000 µg/mL, data not shown).

The *in vitro* tested ToxPI positive chemicals (BAA, Coumarin, Catechol, Quinoline) all varied in the number of "hits" for the incorporated assays. BAA and catechol had the highest amount of assay "hits" with catechol having slightly more than BAA. BAA's higher ToxPI score was predominantly based on its ability to have hits in all five of the biological process in addition to having the most sensitive AC_{50} value. The average AC_{50} value for each tested ToxPI positive constituent ranged from 14 µM- 67 µM, however, when converted into micrograms per microliter this discrepancy diminished, and all ToxPi positive tested chemicals fell within a 10 microgram per microliter range of each other.

This small threshold could explain why ToxPI positive chemicals H9 hESC IC_{50} values were similar despite having different ToxPI predictive chart sizes. This would also suggest that our ToxPI positive visualizations are more an indicator on the likelihood of producing a cytotoxic event within a given concentration range rather than a ranking system for potent cytotoxic constituents.

There was an uncanny consistency between the Toxcast data that was implemented into the ToxPI GUI. For all ToxPI positive predictive charts there was not a reliable assay that provided a hit among the predictive constituents even among each of the biological processes. This variability did not inhibit the ability to predict cytotoxic effects. Though, it would be beneficial to include validated assays such as the MTT for cell death or Bromodeoxyuridine (BrdU) for cell proliferation. Because the Toxicity Forecaster data was generated using high-throughput screening these may not be feasible options as most of the assays were luminescence based and automated, but including data from these assays when available, as well as incorporating data from previous studies could provide stronger confidence in ToxPI predictions. The incorporation of previously reported data in conjunction with Toxcast data has been successful in ranking chemical constituents based on ability to reduce gill size in zebrafish.[33]

Our only ToxPI null predicted chemical to produce a half-maximal value was the most famous chemical constituent in tobacco and tobacco related products: nicotine. Nicotine is a powerful neurotoxin that interacts with acetylcholine receptors and can alter brain development, though its effects are

largely dependent on duration, dose, and habitual use.[40-42] Nicotine has been shown to have dose-dependent inhibition on cell viability and proliferation for a variety of tissues[43] though there are conflicting studies regarding the ability of nicotine to impede cell viability. However, in non-neural cells it can activate antagonistic cell survival and death pathways, though the precise mechanism of choosing one biological process over another is not clear.[44] This can resolve the discrepancy between contradicting results of the cytotoxicity associated with nicotine and explain why both our adult and immature cell viabilities were maintained through all tested concentrations.

In contrast, the role nicotine plays in osteogenesis is transparent as its dose-dependent inhibition is documented in a variety of studies.[45-47] Though ToxPI had a variety of parameters to predict the cytotoxicity of nicotine, osteogenic endpoints were not able to be integrated into the ToxPI predictive model. Therefore, differentiation inhibition did not produce a visualization on the ToxPI chart of nicotine in contrast to our EST *in vitro* data.

EST Biostatistical Model Versus ToxPI Predictions

All *in vitro* tested chemicals were incorporated into the EST bio-statistical model. The model then classified each of the compounds based on their ability to induce embryotoxicity. This classification gave insight into little known effects of a chemical's exposure. Alongside each chemical in the FDA's HPHC list are categories that classify each chemical as a Carcinogen (CA), Respiratory

Toxicant (RT), Cardiovascular Toxicant (CT), Reproductive or Developmental Toxicant (RDT), or Addictive (AD).[48] All tested chemicals were given a CA classification on the HPHC list except for nicotine, that was classified as both an AD and RDT. Our data suggests that in addition to a CA classification both quinoline and catechol are RDTs. This is especially alarming as our H9 hESC IC_{50} catechol levels can be reasonably reached from smoking 1-2 cigarettes.[49] Nicotine was calculated to have an H9 hESC ID_{50} value with no changes in cell viability for the immature and mature cell lines but was listed as a non-embryotoxic compound. Embryotoxicity in the EST is defined as the adverse effects on the embryo expressed as embryonic cell death to one or more body systems that can be expanded to maternal health. This is a limitation of the EST, though it can classify embryotoxic effects the EST biostatistical model cannot classify chemicals who are teratogenic at sub-toxic levels.[50]

ToxPI predicted AC_{50} and *in vitro* h9 hESC's IC_{50} values corresponded well with numerous in *vivo* tests. Coumarin's toxicity in zebrafish[51] and Xenopus[52] provided half-maximal activity values for viability that were adjacent to both our own hESC and hFF IC_{50}. Likewise, quinoline is reported to induce a variety of malformations and toxicity between 29-95 ug/mL depending on the developmental stage of Xenopus[53] where the median lethal dose for other aquatic species has been reported to be 11 ug/mL.[54] Catechol had a variety of animal models[55,56] with toxic concentrations similar to our own and it corroborated with other independent *in vitro* data.[57] BAA also had exposure

values that resulted in the death of zebrafish larvae slightly lower than our results.[58]

For our tested ToxPI null chemicals none of our concentrations were detrimental to cell viability of our H9 hESC. Cotinine levels in blood of chronic smokers is 500 ng/mL, light smokers are from 30-50 ng/mL, whereas 1-10 ng/mL and concentrations below the 1 ng/mL threshold are regarded as low.[59] Our study tested far above these biologically relevant thresholds and found no inhibitory effects. Urethane (ethyl carbamate) in other toxicological studies only induced a reduction in cell viability at excessively high concentrations.[60] These concentrations however are a thousand times greater than can be encountered.[61] Acrylamide exposure for rat and murine NR-50 levels (midpoint toxicity)[62] were relatively close to our IC_{50} values when excluding ToxPI maximum threshold for both H9 and hFF cells. Acrylamide's cytotoxicity in this concentration range seems to be prevalent for both *in vitro* and *in vivo* studies using a variety of animal models.[63,64] Though the estimated dietary concentration of acrylamide is around 1µm for the average adult[65] and additional acrylamide exposure in cigarettes raises the dietary levels by only three times the amount.[66] Though our data suggests a differentiation inhibition capability of nicotine during osteogenesis these levels are not biologically relevant as they are not achieved in arterial blood[67] after smoking and in extreme cases are as high as 0.1 µg/mL.[68-70]

Overall, ToxPI predictions based on the parameters we have set forth are likely indicators of reduced H9 cell viability and can partition between chemicals that induce and do not induce cytotoxic events when tested in ToxPI predictive thresholds. ToxPI may lack sensitivity to detect sub-toxic effects, but as implemented in our study lacks a predictive component for osteogenesis. Though, our parameters may be altered to incorporate genes and pathways that can predict the inhibition of other differentiation processes that are available on the Toxicity Forecaster database. There are potential pitfalls that can arise from the ToxPI system, however, with an ever-growing database and subsequent improvements it can be a useful resource in assessing the ability of a chemical to impact early embryonic development.

THS EST and Combination Testing

THS as a new emerging threat to human health has garnered much attention in the last decade.[71] The main source of THS is attributed to nicotine as it is absorbed by the surface and reacts with nitrous acid (HONO) species in addition to ultraviolet light and other ambient species.[72] However, this is not applicable to all THS constituents as NAT is a non-nicotine derived tobacco constituent that is primarily derived from anatabine and anabasine. THS extracts from carpets exposed to cigarette smoke have confirmed the presence of NNK, NNA, NAT, and NFN.[37] Each of the chemicals were found to have increased concentrations as smoking persisted and found the highest concentrations of

THS constituents were found at 12 months of exposure. Surprisingly, THS constituents are not exclusive to cigarette combustion. Studies have shown that NNN and NNK concentrations were higher in homes occupied by smokeless tobacco users than in tobacco-free homes.[73] This is alarming as THS levels seem to increase with the use of tobacco products regardless of how the products is consumed. This also raises new concerns as cleaning methods such as vacuuming are ineffective in the removal of THS constituents from the environment.

Early efforts into the potential health outcomes of THS focused on genotoxicity and carcinogenicity. These early studies reported THS constituents NNN and NNK to induce DNA damage in human cells at biologically relevant concentrations and subsequently led to their classification as carcinogens.[74] Furthermore, *in vivo* studies have shown THS to reduce the weight and immunity of mice in the absence of carcinogenicty.[75] There have been several attempts to assess the toxicity of THS constituent's *in vitro* as THS terry cloth extracts have demonstrated the ability to inhibit mouse neural stem cell survival as well as mature human fibroblast.[76] NNK has also demonstrated the ability to inhibit lung tissue repair, though there are no experiments that have solely focused on a specific developmental process. To our knowledge we are the first to test the toxicity of NFN and NAT, and Nicotelline using a differentiation protocol.

Three of our THS constituents (NAT, NFN, NNK) did not hinder cell viability or differentiation in the tested concentrations. This suggests that the

screened THS constituents may be non-embryotoxic compounds. Individually, the tested THS constituents themselves may not be cytotoxic but there is strong evidence that THS possess combinatorial effects. For example, NNK synergistically reacts with NNN to produce deleterious effects increasing their capability to induce double strand DNA breaks.[77] Like many chemical concoctions, THS effects appear to be dose-dependent but its effects on various development processes are still not clear. NNA produced a decrease in cell viability for hESC suggesting embryotoxicity at relatively low concentrations. This inhibition of cell viability is within range of NNA concentrations found in the homes of continuous smokers, where these reported findings gave NNA concentrations modest estimations.[78]

Further studies should be done to assess the synergistic effects of THS during embryogenesis. Our lab has done early experiments that suggest many chemicals constituents exhibit a stronger effect on development when used in a ternary combination. Though the full spectrum of the ability of THS to cause potential harm during pregnancy and the early years of childhood are not fully known, we have demonstrated that the THS constituent NNA poses a potential health concern other than carcinogenicity.

CHAPTER SIX

CONCLUSIONS

A Framework for Toxicity Testing in the Future

Narrowing down the primary drivers of the chemical mixture that encompasses tobacco products and smoke remains a large challenge. This study has found that using the ToxPI program in conjunction with Toxcast data can partition cytotoxic constituents from those that will produce no harm within their predictive range. This is especially useful as many tobacco constituents are encountered in the agricultural and pharmaceutical sector. Furthermore, because our parameters inserted into the ToxPI GUI were broad, they can be applied to various products who are made up of a concoction of chemicals and is not limited to those chemicals in tobacco products and smoke. Though the parameters chosen to generate the ToxPI charts were not specific to the osteogenic lineage, their testing in a well-established protocol was a recapitulation of osteogenic development during gastrulation. With the assimilation of Toxcast data in its infancy, the database has the potential to grow and could have data available in the future to help predict osteogenic maldevelopment specifically as seen currently with other target tissues.

With the limitations of available data for HPHC chemicals and the emergence of a new potential threat in the form of THS we found it of great importance to test constituents through the osteogenic protocol. Our data

suggests that the tested THS constituents individually are not all cytotoxic but could still pose great harm in tandem with other tobacco related chemicals. Overall, because there are many routes of exposure to tobacco products even among non-users, it is of importance to incorporate data when available from high-throughput sources to make conclusions about the toxicity and developmental effects a chemical constituent can produce.

REFERENCES

1. Pruss-Usten, A., & Corvalan, C. 2006. Preventing disease through healthy environments. World Health Organization.

2. Wu, S., Legido, A., & De Luca , F. 2004. Effects of valproic acid on longitudinal bone growth. Journal of Child Neurology, 26-30. doi:10.1177/08830738040190010501l

3. Soprano, D. R., & Soprano, K. J. 1995. Retinoids as teratogens. Annual Review, 15, 111-132.

4. The health consequences of smoking—50 years of progress: a report of the surgeon general. Centers for Disease Control and Prevention, 2004. U.S. Department of Health and Human Services, Atlanta. Retrieved January 2018

5. Xu, X., Bishop, E. E., Kennedy, S. M., Simpson, S. A., & Pechacek, T. F. 2015. Annual healthcare spending attributable to cigarette smoking: an update. American Journal of Preventive Medicine, 48(3), 326–333. http://doi.org/10.1016/j.amepre.2014.10.012

6. Smoking and bone health. 2016, May. Retrieved from National Institute of Arthritis and Musculoskeletal and Skin Diseases.

7. Curtin, S. C., & Mathews, T. 2016. Smoking prevalence and cessation before and during pregnancy: Data from birth certificate.2014 National Vital, 65 (1).

8. Rasmussen, S. A. 2012. Human teratogens update 2011: can we ensure safety during pregnancy? Birth Defects Research. Part A, Clinical and Molecular Teratology, 94(3), 123–128. http://doi.org/10.1002/bdra.22887

9. Gilbert SF. Developmental biology. 6th edition. Sunderland (MA): Sinauer Associates; 2000. Available from: https://www.ncbi.nlm.nih.gov/books/NBK9983/

10. Shahi, M., Peymani, A., & Sahmani, M. 2017. Regulation of bone metabolism. Reports of Biochemistry & Molecular Biology, 5(2), 73–82.

11. OpenStax, Anatomy & physiology. Chapter 6.4 bone formation and development OpenStax CNX. Feb 26, 2016 http://cnx.org/contents/14fb4ad7-39a1-4eee-ab6e-3ef2482e3e22@8.24.

12. Cordero, J. F. 1994. Finding the causes of birth defects. The New England Journal of Medicine (331), 48-49. doi:10.1056/NEJM199407073310112

13. Zhang, W., Sui, Y., Ni, J., & Yang, T. 2016. Insights into the nanog gene: a propeller for stemness in primitive stem cells. International Journal of Biological Sciences, 12(11), 1372–1381. http://doi.org/10.7150/ijbs.16349

14. Boyer LA, Lee TI, Cole MF, et al. 2005. Core transcriptional regulatory circuitry in human embryonic stem cells. Cell;122(6):947-956. doi:10.1016/j.cell.2005.08.020.

15. Loh YH, Wu Q, Chew JL, Vega VB, Zhang W, Chen X, et al. 2006. The Oct4 and nanog transcription network regulates pluripotency in mouse embryonic stem cells. Nat Genet;38(4):431–440. doi: 10.1038/ng1760.

16. Metzger, J. M., W.-I. Lin, R. A. Johnston, M. V. Westfall, and L. C. Samuelson. 1995. Myosin heavy chain expression in contracting myocytes isolated during embryonic stem cell cardiogenesis. Circulation Research 76.5: 710-19.

17. Jiang, N., Chen, M., Yang, G., Xiang, L., He, L., Hei, T. K., … Mao, J. J. 2016. Hematopoietic stem cells in neural-crest derived bone marrow. Scientific Reports, 6, 36411. http://doi.org/10.1038/srep36411

18. Russell WMS, Burch RL. 1959. (as reprinted 1992). The principles of humane experimental technique. Wheathampstead (UK): Universities Federation for Animal Welfare.

19. Tannenbaum, J., & Bennett, B. T. 2015. Russell and Burch's 3Rs then and now: The need for clarity in definition and purpose. Journal of the American Association for Laboratory Animal Science: JAALAS, 54(2), 120–132.

20. Spielmann H, Pohl I, Doring B, Liebsch m, Moldenbauer F. 1997. The embryonic stem cell test (EST), an in vitro embryotoxicity test using two permanent cell lines: 3T3 fibroblasts and embryonic stem cells. In Vitro Toxicology. 10:119–27.

21. Genschow E, Spielmann H, Scholz G, Seiler A, Brown N, Piersman A, Brady M, Clemann N, Huuskonen H, Pailard F, Bremer S, Becker K. 2002. The ECVAM international validation study on in vitro embryotoxicity tests: results of the definitive phase and evaluation of prediction models. European Centre for the Validation of Alternative Methods. Alternatives to Laboratory Animals. 30(2):151-76.

22. Genschow E, Spielmann H, Scholz G, Pohl I, Seiler A, Clemann N, Bremer S, Becker K. 2004. Validation of the embryonic stem cell test in the international ECVAM validation study on three in vitro embryotoxicity tests. Alternatives to Laboratory Animals. 32(3):209-44.

23. Sparks, N. R.L. and zur Nieden, N. I. 2014. Pluripotent stem cells as tools to assess developmental toxicity: diversity instead of consolidation, in handbook of nanotoxicology, Nanomedicine and Stem Cell Use in Toxicology (eds S. C. Sahu and D. A. Casciano), John Wiley & Sons, Ltd, Chichester, UK. doi: 10.1002/9781118856017.ch16

24. zur Nieden N.I., Kempka G., Ahr H.J. 2003. In vitro differentiation of embryonic stem cells into mineralized osteoblasts. Differentiation. 71(1):18-27.

25. zur Nieden NI, Kempka G, Rancourt DE, Ahr HJ. 2005. Induction of chondro-, osteo- and adipogenesis in embryonic stem cells by bone morphogenetic protein-2: effect of cofactors on differentiating lineages. BMC Developmental Biology. 5:1.

26. zur Nieden N., Kempka G., Ahr H. 2004. Molecular multiple endpoint embryonic stem cell test—A possible approach to test for the teratogenic potential of compounds. Toxicol. Appl. Pharmacol. 194:257–269. doi: 10.1016/j.taap.2003.09.019

27. Taube S, zur Nieden N.I, 2007. Steering embryonic stem cell fate towards osteoblasts with downstream non-canonical Wnt targets in vitro. J Stem Cells Regen Med. May 16;2(1):132

28. Zur Nieden, N.I, Ruf, L.J., Kempka,G., Hildebrand, Ahr, H.J., 2001. Molecular markers in embryonic stem cells. Toxicol. In Vitro 15, 455-461

29. Walker, L., Baumgartner, L., Keller, K. C., Ast, J., Trettner, S., & zur Nieden, N. I. 2015. Non-human primate and rodent embryonic stem cells are differentially sensitive to embryotoxic compounds. Toxicology Reports, 2, 165–174. http://doi.org/10.1016/j.toxrep.2014.11.016

30. Reif, David M. et al. 2010. Endocrine profiling and prioritization of environmental chemicals using Toxcast data. Environmental Health Perspectives 118.12 (2010): 1714–1720. PMC.

31. Reif, D. M., Sypa, M., Lock, E. F., Wright, F. A., Wilson, A., Cathey, T., … Rusyn, I. 2013. ToxPI GUI: an interactive visualization tool for transparent integration of data from diverse sources of evidence. Bioinformatics, 29(3), 402–403. http://doi.org/10.1093/bioinformatics/bts686

32. Filer D., Patisaul H.B., Schug T., Reif D., Thayer K. 2014. Test driving ToxCast: endocrine profiling for 1858 chemicals included in phase II. Current opinion in pharmacology.19:145-152. doi:10.1016/j.coph

33. Kleinstreuer N.C., Judson R.S., Reif D.M., et al. 2011. Environmental impact on vascular development predicted by high-throughput screening. Environmental Health Perspectives.119(11):1596-1603. doi:10.1289/ehp.1103412.

34. Janesick A.S., Dimastrogiovanni G., Vanek L., et al. 2016. On the utility of Toxcast and ToxPI as methods for identifying new obesogens. Environmental Health Perspectives. 24(8):1214-1226. doi:10.1289/ehp.1510352.

35. Auerbach, S., Filer, D., Reif, D., Walker, V., Holloway, A. C., Schlezinger, J., … Thayer, K. A. 2016. Prioritizing environmental chemicals for obesity and diabetes outcomes research: a screening approach using Toxcast high-throughput data. Environmental Health Perspectives, 124(8), 1141–1154. http://doi.org/10.1289/ehp.1510456

36. Family smoking prevention and tobacco control act. http://www.fda.gov/TobaccoProducts/GuidanceComplianceRegulatoryInformation/ucm237092.htm 2009. Accessed on 21 Jan 2016.

37. Bahl, V., Jacob, P., Havel, C., Schick, S. F., & Talbot, P. 2014. Thirdhand cigarette smoke: factors affecting exposure and remediation. PLoS ONE, 9(10), e108258. http://doi.org/10.1371/journal.pone.0108258

38. Ducharme N.A., Peterson L.E., Benfenati E., Reif D., McCollum C.W., Gustafsson JA, Bondesson M. 2013. Meta-analysis of toxicity and teratogenicity of 133 chemicals from zebrafish developmental toxicity studies. Reprod Toxicol. 41:98–108. doi: 10.1016/j.reprotox.2013.06.070.

39. Janesick, A. S., Dimastrogiovanni, G., Vanek, L., Boulos, C., Chamorro-García, R., Tang, W., & Blumberg, B. 2016. On the utility of Toxcast and ToxPI as methods for identifying new obesogens. Environmental Health Perspectives, 124(8), 1214–1226. http://doi.org/10.1289/ehp.1510352

40. Lindley A.A., Becker S., Gray R.H., Herman A.A. 2000. Effect of continuing or stopping smoking during pregnancy on infant birth weight, crown-heel length, head circumference, ponderal index, and brain: body weight ratio. Am. J. Epidemiol. 152:219–225.

41. Bruin, J. E., Gerstein, H. C., & Holloway, A. C. 2010. Long-term consequences of fetal and neonatal nicotine exposure: A critical review. Toxicological Sciences, 116(2), 364–374. http://doi.org/10.1093/toxsci/kfq103

42. Ross E.J., Graham D.L., Money K.M., Stanwood G.D. 2015. Developmental consequences of fetal exposure to drugs: what we know and what we still must learn. Neuropsychopharmacology. 40(1):61-87. doi:10.1038/npp.2014.147

43. Holbrook, B. D. 2016. The effects of nicotine on human fetal development. Birth Defect Res C, 108: 181–192. doi:10.1002/bdrc.21128

44. Wessler, I., & Kirkpatrick, C. J. 2008. Acetylcholine beyond neurons: the non-neuronal cholinergic system in humans. British Journal of Pharmacology, 154(8), 1558–1571. http://doi.org/10.1038/bjp.2008.185

45. Tanaka, H., Tanabe, N., Kawato, T., Nakai, K., Kariya, T., Matsumoto, S., … Maeno, M. 2013. Nicotine affects bone resorption and suppresses the expression of cathepsin K, MMP-9 and vacuolar-type H^+ ATPase D2 and actin organization in osteoclasts. PLoS ONE, 8(3), e59402. http://doi.org/10.1371/journal.pone.0059402

46. Kim B.S., Kim S.J., Kim H.J., Lee S.J., Park Y.J., Lee J., et al. 2012. Effects of nicotine on proliferation and osteoblast differentiation in human alveolar bone marrow-derived mesenchymal stem cells. Life Sci. 90:109–115.

47. Chang Y.C., Huang F.M., Tai K.W., Yang L.C., Chou M.Y. 2002. Mechanisms of cytotoxicity of nicotine in human periodontal ligament fibroblast cultures in vitro. J Periodontal Res. 37:279–285.

48. US Food and Drug Administration. Harmful and potentially harmful constituents in tobacco products and tobacco smoke; established list, federal register. 2012. pp. 20034–20037.

49. Hecht S.S., Carmella S., Mori H., Hoffmann D. 1981. Role of catechol as a major cocarcinogen in the weakly acidic fraction of smoke condensate. J Natl Cancer Inst. 66:163–169.

50. Riebeling C., Hayess K., Peters A.K., Steemans M., Spielmann H., Luch A., Seiler A.E. 2012. Assaying embryotoxicity in the test tube: current limitations of the embryonic stem cell test (EST) challenging its applicability domain. Crit Rev Toxicol 42:443–464.

51. Weigt S, Huebler N, Strecker R, Braunbeck T, Broschard TH. 2012. Developmental effects of coumarin and the anticoagulant coumarin derivative warfarin on zebrafish (Danio rerio) embryos. Reproductive Toxicology. 33(2):133–141. doi: 10.1016/j.reprotox.2011.07.001.

52. Fort D.J., Stover E.L., Propst T., Hull M.A., Bantle J.A. 1998. Evaluation of the developmental toxicities of coumarin, 4-hydroxycoumarin, and 7-hydroxycoumarin using FETAX. Drug Chem Toxicol. 24:2,103-115

53. K. R. Davis, T. W. Schultz, J. N. Dumont. 1981. Toxic and teratogenic effects of selected aromatic amines on embryos of the amphibian xenopus laevis. Arch Environ Contam Toxicol.10(3): 371–391.

54. Black J. A., Birge W. J.,Westerman A. G, Francis P. C. 1983. Comparative aquatic toxicology of aromatic hydrocarbons. Fundam Appl Toxicol. Sep-Oct; 3(5): 353–358.

55. Taysse L., Troutaud D., Khan N., Deschaux P. 1995. Structure-activity relationship of phenolic compounds (phenol, pyrocatechol and hydroquinone) on natural lymphocytotoxicity of carp (cyprinus carpio). Toxicol. 98, 207–214. 10.1016/0300-483X(94)03011-P

56. Tsutsui T, Hayashi N, Maizumi H, Huff J, Barrett J.C. 1997. Benzene-, catechol-, hydroquinone- and phenol-induced cell transformation, gene mutations, chromosome aberrations, aneuploidy, sister chromatid exchanges and unscheduled DNA synthesis in Syrian hamster embryo cells. Mutat Res. 1997;373(1):113–23. doi: 10.1016/S0027-5107(96)00196-0

57. McCue J.M., Lazis S, Cohen J.J., Modiano J.F., Freed B.M. 2003. Hydroquinone and catechol interfere with T cell cycle entry and progression through the G1 phase. Mol immunol. 39(16):995–1001. doi: 10.1016/S0161-5890(03)00046-4.

58. Goodale, B. C., Tilton, S. C., Wilson, G., Corvi, M. M., Janszen, D. B., Anderson, K. A., … Tanguay, R. L. 2013. Structurally distinct polycyclic aromatic hydrocarbons induce differential transcriptional responses in developing zebrafish. Toxicology and Applied Pharmacology, 272(3), 656–670. http://doi.org/10.1016/j.taap.2013.04.024

59. Hukkanen J, Jacob P, Benowitz N.L. 2005. Metabolism and disposition kinetics of nicotine. Pharmacol. Rev. 57:79–115. doi: 10.1124/pr.57.1.3

60. Balharry D., Sexton K., BéruBé K.A. 2008. An in vitro approach to assess the toxicity of inhaled tobacco smoke components: nicotine, cadmium, formaldehyde and urethane. Toxicology. 244:66–76. doi: 10.1016/j.tox.2007.11.001.

61. Liu, H., Cui, B., Xu, Y., Hu, C., Liu, Y., Qu, G., . . . Shi, J. 2017. Ethyl carbamate induces cell death through its effects on multiple metabolic pathways. Chemico-Biological Interactions, 277, 21-32. doi:10.1016/j.cbi.2017.08.008

62. Borenfreund E, et al. 1987. In vitro cytotoxicity of heavy metals, acrylamide, and organotin salts to neural cells and fibroblasts.Cell Biol Toxicol. 3(1):63-73.

63. Wei Q, Li J, Li X, Zhang L, Shi F. 2014. Reproductive toxicity in acrylamide-treated female mice. Reprod Toxicol. 46:121–128. doi: 10.1016/j.reprotox.2014.03.007.

64. LoPachin, R. M., & Gavin, T. 2012. Molecular mechanism of acrylamide neurotoxicity: lessons learned from organic chemistry. Environmental Health Perspectives, 120(12), 1650–1657. http://doi.org/10.1289/ehp.1205432

65. Walters B., Hariharan V., Huang H. 2014. Dietary levels of acrylamide affect rat cardiomyocyte properties Food Chem. Toxicol., 71,68-73

66. Olesen, P.T.; Olsen, A; Frandsen, H; Frederiksen, K; Overvad, K; Tjønneland, A. 2008. Acrylamide exposure and incidence of breast cancer among postmenopausal women in the Danish Diet, Cancer and Health Study. International Journal of Cancer. 122 (9): 2094–100. doi:10.1002/ijc.23359.

67. Gourlay SG, Benowitz NL. 1987. Arteriovenous differences in plasma concentration of nicotine and catecholamines and related cardiovascular effects after smoking, nicotine nasal spray, and intravenous nicotine. Clin Pharmacol Ther. 62(4):453-63.

68. Henningfield JE, Keenan RM. 1983. Nicotine delivery kinetics and abuse liability. J Consult Clin Psychol. 61(5):743-50.

69 Lunell E, Molander L, Ekberg K, Wahren J. 2000. Site of nicotine absorption from a vapour inhaler--comparison with cigarette smoking. Eur J Clin Pharmacol. 55(10):737-41.

70. Rose JE, Behm FM, Westman EC, Coleman RE. 1999. Arterial nicotine kinetics during cigarette smoking and intravenous nicotine administration: implications for addiction. Drug Alcohol Depend. 56(2):99-107.

71. Rabin R.B. 2009. A new cigarette hazard: third-hand smoke.; The New York Times. Available online:

http://www.nytimes.com/2009/01/03/health/research/03smoke.html?_r=1&em=&pagewanted=print.

72. Sleiman M., Gundel L.A., Pankow J.F., Jacob P., III, Singer B.C., Destaillats H. 2010. Formation of carcinogens indoors by surface-mediated reactions of nicotine with nitrous acid, leading to potential thirdhand smoke hazards. Proc. Natl. Acad. Sci. USA.107:6576–6581. doi: 10.1073/pnas.0912820107.

73. Whitehead, T. P., Havel, C., Metayer, C., Benowitz, N. L., & Jacob, P. 2015. Tobacco alkaloids and tobacco-specific nitrosamines in dust from homes of smokeless tobacco users, active smokers, and non-tobacco. Chemical Research in Toxicology, 28(5), 1007–1014. http://doi.org/10.1021/acs.chemrestox.5b00040

74. Hecht, S. S. 2008. Progress and challenges in selected areas of tobacco carcinogenesis. Chemical Research in Toxicology, 21(1), 160–171. http://doi.org/10.1021/tx7002068

75. Hang B., Snijders A.M., Huang Y., Schick S.F., Wang P., Xia Y., Havel C., Jacob P., III, Benowitz N., Destaillats H., et al. 2017 Early exposure to thirdhand cigarette smoke affects body mass and the development of immunity in mice. doi: 10.1038/srep41915.

76. Bahl, V., Shim, H. J., Jacob, P., Dias, K., Schick, S. F., & Talbot, P. 2016. Thirdhand smoke: chemical dynamics, cytotoxicity, and genotoxicity in outdoor and indoor environments. Toxicology in Vitro : An International Journal Published in Association with BIBRA, 32, 220–231. http://doi.org/10.1016/j.tiv.2015.12.007

77. Hang, B., Sarker, A. H., Havel, C., Saha, S., Hazra, T. K., Schick, S., … Gundel, L. A. 2013. Thirdhand smoke causes DNA damage in human cells. Mutagenesis, 28(4), 381–391. http://doi.org/10.1093/mutage/get013

78. Jacob, P., Benowitz, N. L., Destaillats, H., Gundel, L., Hang, B., Martins-Green, M., … Whitehead, T. P. 2017. Thirdhand smoke: new evidence, challenges, and future directions. Chemical Research in Toxicology, 30(1), 270–294. http://doi.org/10.1021/acs.chemrestox.6b00343